



Environmental fluoxetine promotes skin cell proliferation and wound healing[☆]

Quentin Rodriguez-Barucg^a, Angel A. Garcia^a, Belen Garcia-Merino^{a,b}, Tomilayo Akinmola^a, Temisanren Okotie-Eboh^a, Thomas Francis^a, Eugenio Bringas^b, Inmaculada Ortiz^b, Mark A. Wade^a, Adam Dowe^c, Domino A. Joyce^d, Matthew J. Hardman^a, Holly N. Wilkinson^a, Pedro Beltran-Alvarez^{a,*}

^a Biomedical Institute for Multimorbidity, Centre for Biomedicine, Hull York Medical School, University of Hull, Cottingham Rd, HU6 7RX, Hull, UK

^b Department of Chemical and Biomolecular Engineering, ETSIT, University of Cantabria, Av Castros s/n, 39005, Santander, Spain

^c Metabolomics & Proteomics Laboratory, Bioscience Technology Facility, Department of Biology, University of York, Wentworth Way, York, YO10 5DD, UK

^d Evolutionary and Ecological Genomics Group, School of Natural Sciences, University of Hull, Cottingham Rd, HU6 7RX, Hull, UK

ARTICLE INFO

Keywords:

Fluoxetine
Keratinocyte
Serotonin
Skin
Wound healing

ABSTRACT

This study investigates the effects of environmentally-relevant concentrations of fluoxetine (FLX, commercial name: Prozac) on wound healing. Pollution of water systems with pharmaceutical and personal care products, including antidepressants such as FLX and other selective serotonin reuptake inhibitors, is a growing environmental concern. Environmentally-relevant FLX concentrations are known to impact physiological functions and behaviour of aquatic animals, however, the effects of exposure on humans are currently unknown. Using a combination of human skin biopsies and a human keratinocyte cell line, we show that exposure to environmental FLX promotes wound closure. We show dose-dependent increases in wound closure with FLX concentrations from 125 ng/l. Using several -omics and pharmaceutical approaches, we demonstrate that the mechanisms underlying enhanced wound closure are increased cell proliferation and serotonin signalling. Transcriptomic analysis revealed 350 differentially expressed genes after exposure. Downregulated genes were enriched in pathways related to mitochondrial function and metabolism, while upregulated genes were associated with cell proliferation and tissue morphogenesis. Kinase profiling showed altered phosphorylation of kinases linked to the MAPK pathway. Consistent with this, phosphoproteomic analyses identified 235 differentially phosphorylated proteins after exposure, with enriched GO terms related to cell cycle, division, and protein biosynthesis. Treatment of skin biopsies and keratinocytes with ketanserin, a serotonin receptor antagonist, reversed the increase in wound closure observed upon exposure. These findings collectively show that exposure to environmental FLX promotes wound healing through modulating serotonin signalling, gene expression and protein phosphorylation, leading to enhanced cell proliferation. Our results justify a transition from the study of behavioural effects of environmental FLX in aquatic animals to the investigation of effects of exposure on wound healing in aquatic and terrestrial animals, including direct impacts on human health.

1. Introduction

Pollution of freshwaters with pharmaceuticals and personal care products poses a real threat to environmental and human health (Blair et al., 2013; Brooks et al., 2005; Cizmas et al., 2015; Daughton & Ternes,

1999). One example of environmentally relevant pharmaceuticals is antidepressants. Fluoxetine (FLX, commercial brand name: Prozac) is a selective serotonin reuptake inhibitor (SSRI) widely prescribed for the treatment of mental health and mood disorders, including depression, obsessive-compulsive disorder and panic disorder (Gosmann et al.,

Abbreviations: 5-HT, 5-hydroxytryptamine, or serotonin; ER, environmentally relevant; FLX, fluoxetine; GO, gene ontology; MAPK, mitogen-activated protein kinase; SSRI, selective serotonin reuptake inhibitor.

[☆] This paper has been recommended for acceptance by Yaoyu Zhou.

* Corresponding author.

E-mail address: p.beltran-alvarez@hull.ac.uk (P. Beltran-Alvarez).

<https://doi.org/10.1016/j.envpol.2024.124952>

Received 18 June 2024; Received in revised form 21 August 2024; Accepted 12 September 2024

Available online 12 September 2024

0269-7491/© 2024 The Authors. Published by Elsevier Ltd. This is an open access article under the CC BY license (<http://creativecommons.org/licenses/by/4.0/>).

2021). After ingestion, FLX is partly metabolised to the active nor-fluoxetine and other metabolites which, together with unmodified FLX, are then excreted through urine (Edinoff et al., 2021; Vaswani et al., 2003). Wastewater treatment plants are not efficient at removing FLX and its metabolites (Blair et al., 2013; Brooks et al., 2005; Salahi-nejad et al., 2022; Silva et al., 2012) and, as a result, FLX concentrations in the hundreds of ng/l can build up in freshwater systems, making FLX a priority contaminant in ecotoxicology (Lyu et al., 2019; Santos et al., 2013; Silva et al., 2012; Silva et al., 2015).

Indeed, exposure to environmentally-relevant (ER) FLX concentrations has effects on the behaviour of many vertebrate and invertebrate freshwater species, such as crustaceans and fish. These effects include altered physiological function and behaviour and can have a negative impact on growth, reproduction, and population success (Bertram et al., 2018; Bossus et al., 2014; De Castro-Catala et al., 2017; Ford & Fong, 2016; Guler & Ford, 2010; Martin et al., 2019; Prasad et al., 2015; Weinberger & Klaper, 2014). Of note, this impact is likely to increase in the 21st century due to population growth, urbanisation and climate change-induced water scarcity, which can cause increased FLX concentrations in local and regional freshwater systems (Cizmas et al., 2015; Schlusener et al., 2015). FLX has been found in the aquatic environment near wastewater plants at concentrations of 0.4–3645 ng/l and in surface waters and groundwaters at concentrations of 0.5–596 ng/l (Batt et al., 2008; Cizmas et al., 2015; Correia et al., 2023; Gros et al., 2009; Grzesiuk et al., 2023; Schlusener et al., 2015; Sousa et al., 2011; Tan et al., 2020; Vasskog et al., 2006). Mechanistically, FLX (and other SSRI such as sertraline) blocks the serotonin (5-HT) transporter and thus 5-HT clearance from the synaptic cleft, rising extracellular 5-HT concentrations (Coleman et al., 2016; Tate et al., 2021). Serotonin-mediated signalling is regulated through 5-HT receptors (5-HTR), of which seven distinct families are encoded for in the human genome, known as 5-HTR₁₋₇. Mostly by coupling to G proteins, 5-HTRs cascade downstream signalling through a range of evolutionary conserved pathways, regulated by protein kinases (notably mitogen-activated protein kinases, MAPK) and protein phosphorylation, which ultimately control cell fate, growth and proliferation (Sahu et al., 2018).

Serotonin receptors and transporters are ubiquitously expressed (Kim et al., 2014) and control 5-HT signalling pathways in a variety of physiological processes, including wound healing (Nguyen et al., 2019; Sadiq et al., 2018). Skin wound healing is the well-coordinated process of restoring skin integrity after injury. Haemostasis is initiated immediately following injury to limit blood loss, and coincides with the recruitment of neutrophils and macrophages during early inflammation. During the proliferative phase, keratinocytes in the epidermis proliferate and migrate from the edges of the wound to close the wound gap, a process known as re-epithelialisation. In this phase (up to 30 days), endothelial cells also form new blood vessels (angiogenesis), and fibroblasts deposit extracellular matrix to form the granulation tissue. A final remodelling phase strengthens the healing tissue resulting in scar formation and maturation, which can last for up to 2 years (Wilkinson & Hardman, 2020).

In the skin, 5-HT receptors have been identified in keratinocytes, melanocytes, leukocytes and fibroblasts (Martins et al., 2020; Nordlind et al., 2008; Slominski et al., 2004). Serotonin receptors can modulate skin inflammation, pigmentation and barrier function, including through regulating cell proliferation (Kim et al., 2018). Prior research has investigated the role of 5-HT and FLX on various models of wound healing, both *in vitro* and *ex vivo*. For example, it has been reported that 5-HT can affect the migration and proliferation of keratinocytes and fibroblasts, which are crucial for re-epithelialisation and the formation of granulation tissue (Nguyen et al., 2019; Sadiq et al., 2018). Serotonin also modulates the inflammatory phase and angiogenesis by impacting cytokine release and leukocyte infiltration (Haub et al., 2010; León-Ponte et al., 2007), and activating kinase (including MAPK) signalling in endothelial cells (Zamani & Qu, 2012), respectively. However, previous

studies have also reported contrasting results. While several groups have shown that treatment with 5-HT enhances the migration of keratinocytes in scratch assays (using cell lines) (Nguyen et al., 2019; Sadiq et al., 2018), the effect of FLX on wound healing is controversial. Topical administration of FLX (0.2–2%, that is, 2–20 g/l) improved wound healing in diabetic mouse skin (Nguyen et al., 2019) and infected wounds (Yoon et al., 2021), but systemic treatment of mice with post-thermal injury with 10 mg/kg FLX suppressed wound re-epithelialisation, including through decreasing keratinocyte proliferation (Sadiq et al., 2018). Moreover, FLX impaired (Sadiq et al., 2018), and enhanced (Nguyen et al., 2019), the migration of keratinocytes in scratch assays. Of note, FLX concentrations used by previous research could potentially be relevant to therapeutic applications of FLX in wound healing, but were orders of magnitude above ER-FLX concentrations. Therefore, a clear knowledge gap currently exists around any effects of ER-FLX concentrations on wound healing.

From the standpoint of the increasing concern about the presence of FLX in freshwaters, and of conflicting evidence pointing towards a role of FLX (at therapeutic concentrations) in wound healing, in this work we set out to investigate any effects of ER-FLX concentrations on wound healing. We used a range of FLX concentrations (62.5–5,400 ng/l) and exposed cell models and human skin biopsies to FLX for up to 48 h. Given the complexity of 5-HT signalling pathways (Sahu et al., 2018), we used -omics technologies to provide an in-depth level of analysis of the effects of exposure. Our overarching hypothesis was that exposure to ER-FLX concentrations promotes wound healing. We specifically hypothesised that: 1) the mechanism underlying wound healing enhancement is increased 5-HT signalling; 2) exposure leads to changes in gene expression and protein phosphorylation associated with increased cell proliferation.

2. Materials and methods

2.1. Cells and clinical samples

HaCaT cells are spontaneously immortalised human keratinocytes from the cultivation of normal human adult skin keratinocytes and were purchased from AddexBio. HaCaT cells have been extensively used as a model system in skin research (Jin et al., 2024; Curtytek et al., 2021; Kim et al., 2018; Mokrzyński & Szweczyk, 2024; Payuhakrit et al., 2024). HaCaT cells were cultured in 5% CO₂ incubators at 37 °C and passaged every 3 days or when at 80% confluence.

All procedures with human samples were performed in compliance with relevant laws and institutional guidelines and were approved by the appropriate institutional committees. Fresh human skin was obtained from patients undergoing elective surgeries under NHS REC approval (17/SC/0220) with written, informed patient consent and using our established protocols (Wilkinson et al., 2021). This work was carried out in accordance with [The Code of Ethics of the World Medical Association](#) (Declaration of Helsinki). Exclusion criteria included factors known to influence wound healing (e.g., nutritional deficiencies, steroid use, advanced age).

2.2. Scratch assays using cells

Cells grown in 24-well polystyrene plates (Sarstedt) were left at 37 °C for three days until a monolayer of cells covered the entirety of each well. Using a 1000 µL pipette tip, a line was scratched through the middle of each well, and cells were exposed to SSRI (FLX or sertraline, at concentrations ranging from 62.5 to 5400 ng/l as indicated in figures), mitomycin C (800 µg/l) and ketanserin (10 µM). For each exposure and treatment condition, at least four biological replicates were done at each of four cell passages. For proliferation assays, we used the Click-iT Edu kit (#BCK-EDU488, Thermo Fisher). Following 28–36 h after scratch (and including a control at time zero), cells were fixed by 1% crystal violet. Comparisons between conditions were done at the same

endpoint. Wells were visualised using a bright field Olympus BX51 microscope with 4× objectives and using CellSens software to capture images. Four pictures of each well were taken. Analysis was done using ImageJ (Schneider et al., 2012) by measuring the area of the scratch at the appropriate time. The percentage of scratch closure was calculated using the formula: $100 - ((\text{wound area at time of measurement} / \text{wound area at time zero}) \times 100)$.

2.3. Wound healing assays using skin biopsies

Ex vivo experiments with skin biopsies have previously been described (Wilkinson et al., 2021). Briefly, skin was placed dermis-side down in a 90 mm sterile Petri dish, and adipose tissue was removed using sterile scissors. Partial thickness wounds were created by pressing a 2 mm biopsy punch against the skin and twisting gently. The 2 mm wound was cut out and removed using forceps and curved iris scissors. A 6 mm biopsy punch was then used to create an explant with the wound in the centre. The wound explants were placed epidermis-side up on a stack of two sterile absorbent pads and a nylon filter membrane in a 60 mm Petri dish containing 4 mL of human skin media (DMEM with 2 mM L-glutamine, 1% (v:v) antibiotic-antimycotic solution, and 10% (v:v) fetal bovine serum), and exposed to/treated with the appropriate FLX and ketanserin concentrations. Explants were cultured at 37 °C and 5% CO₂ for 48 h. Biopsies were then fixed in 4% formaldehyde and stained with an anti-mouse keratin 14 antibody (LL002, Abcam, 1:1,000, overnight). Keratin 14 was detected using a goat anti-mouse Alexa Fluor 488 – conjugated secondary antibody (1:400) and wounds were counterstained using DAPI. Wounds were then imaged using a confocal laser scanning microscope (Zeiss LSM 710) equipped with a 2.5× objective and 405-nm diode and 488-nm argon lasers. Analysis was performed using ImageJ (as previously). The skin samples used in this study were obtained from seven donors (please see below for clinical data). At least four biopsies per donor, per condition were processed as technical replicates.

2.4. RNAseq

HaCaT cells grown in 6-well plates were scratched three times per well and total RNA was isolated after either 6 or 36 h using the Pure-Link™ RNA Mini Kit (#12183020, Thermo Fisher Scientific) following the manufacturer's instructions. Total RNA was analysed to yield the transcriptomic profile of the cells in the four different conditions (exposed to 540 ng/l FLX for 6 and 36 h, and corresponding time controls). For each condition, four biological replicates were done at each of four cell passages. Library preparation and RNA sequencing were done by Novogene Co. Ltd. (Cambridge, UK) using the Illumina NovaSeq 6000 platform. Briefly, the HISAT2 algorithm was used for read alignment and FPKM to normalise gene expression. Differential gene expression was determined from read counts using the DESeq2 R package. Gene expression was log₂ transformed, and the calculated p-values were adjusted using the Benjamini–Hochberg correction for false discovery rate (padj) (Feugere et al., 2022). Genes significantly (padj ≤ 0.05) up- or down-regulated with a gene symbol/ID annotation were used in subsequent analysis.

2.5. Protein microarrays

HaCaT cells were transferred to 6-well plates using three wells per condition (three technical replicates). Cells were incubated at 37 °C until confluence and scratched as described before (three scratches per well were done for these experiments). After 6 or 36 h as appropriate, cells were lysed in 2% SDS. Lysates were centrifuged at 14,000×g for 5 min, and the supernatant was kept for processing. Proteome profiler™ kits (#ARY003C, R&D systems) were used to profile the phosphorylation status on 37 kinases and two related proteins, following the instructions of the manufacturer and based on previous in-house work (Riley et al.,

2021). Blots were developed using Clarity™ ECL western substrate (Bio-Rad) and visualised using a ChemiDoc™ Imaging system (Bio-Rad). Densitometry was done using ImageJ (Schneider et al., 2012). For each condition, four biological replicates were done at each of four cell passages.

2.6. Phosphoproteomics

Cells were grown and scratched as for protein microarrays. Cells were lysed in 9 M urea with 1 mM sodium orthovanadate, 2.5 mM sodium pyrophosphate, 1 mM B-glycerophosphate and protease inhibitors (Complete, Sigma-Aldrich). Proteins were digested using trypsin (Promega) and phosphopeptides were enriched using Zr-IMAC HP-functionalized magnetic microspheres (MR-ZHP002 MagReSyn) following the manufacturer's protocol. Briefly, peptides were resuspended in 0.1 M glycolic acid in 80% (v:v) acetonitrile (ACN) and 5% (v:v) trifluoroacetic acid (TFA) and mixed with 80 μL of equilibrated microspheres. Bound phosphopeptides were washed with aqueous 80% (v:v) ACN containing 1% (v:v) TFA, then aqueous 10% (v:v) ACN containing 0.2% (v:v) TFA, before eluting with aqueous 1% (v:v) ammonium hydroxide. Phosphopeptide-enriched eluent was dried down in a vacuum concentrator and reconstituted in aqueous 0.1% (v:v) TFA for LC-MS/MS analysis. Peptides were loaded onto an mClass nanoflow UPLC system (Waters) equipped with a nanoEase M/Z Symmetry 100 Å C18, 5 μm trap column (180 μm × 20 mm, Waters) and a PepMap, 2 μm, 100 Å, C18 EasyNano nanocapillary column (75 μm × 500 mm, Thermo). The trap wash solvent was aqueous 0.05% (v:v) trifluoroacetic acid and the trapping flow rate was 15 μL/min. The trap was washed for 5 min before switching flow to the capillary column. Separation used gradient elution of two solvents: solvent A, aqueous 0.1% (v:v) formic acid; solvent B, acetonitrile containing 0.1% (v:v) formic acid. The flow rate for the capillary column was 300 nL/min and the column temperature was 40 °C. The linear multi-step gradient profile was: 3–10% B over 7 min, 10–35% B over 30 min, 35–99% B over 5 min and then wash step with 99% solvent B for 4 min. The column was returned to initial conditions and re-equilibrated for 15 min before subsequent injections.

The nanoLC system was interfaced with an Orbitrap Fusion Tribrid mass spectrometer (Thermo) with an EasyNano ionisation source (Thermo) (Marsden et al., 2021a,b). Positive ESI-MS and MS2 spectra were acquired using Xcalibur software (version 4.0, Thermo). Instrument source settings were: ion spray voltage, 1900 V; sweep gas, 0 Arb; ion transfer tube temperature; 275 °C. MS1 spectra were acquired in the Orbitrap with: 120,000 resolution, scan range: m/z 375–1500; AGC target, 4e5; max fill time, 100 ms. Data dependent acquisition was performed in top speed mode using a 1 s cycle, selecting the most intense precursors with charge states >1. Easy-IC was used for internal calibration. Dynamic exclusion was performed for 50 s post precursor selection and a minimum threshold for fragmentation was set at 5e3. MS2 spectra were acquired in the linear ion trap with: scan rate, turbo; quadrupole isolation, 1.6 m/z; activation type, HCD; activation energy: 32%; AGC target, 5e3; first mass, 110 m/z; max fill time, 100 ms. Acquisitions were arranged by Xcalibur to inject ions for all available parallelizable time.

Peak lists in raw format were loaded into PEAKS Studio X Pro (Version 10.6, Bioinformatics Solutions Inc.) for peptide identification and peak area-based label-free relative quantification (Barry et al., 2023). Database searching was performed against the human subset of the SwissProt database appended common proteomic contaminants, specifying: Enzyme, trypsin; Max missed cleavages, 1; Fixed modifications, Carbamidomethyl (C); Variable modifications, Oxidation (M), Phosphorylation (STY), Pyro-glu (EQ), Deamidation (NQ), Peptide tolerance, 3 ppm; MS/MS tolerance, 0.5 Da. Peptide identifications were filtered to 1% false discovery rate as assessed empirically against a decoy database. Label-free relative quantification was performed using the PEAKS-Q module, and pair-wise statistical differences determined using the PEAKS Q significance model.

Additional statistical comparison of relative phosphopeptide abundance between groups was performed using FragPipe-Analyst, run locally using R (4.3.2). Testing used limma (Ritchie et al., 2015), following sample minimum imputation. Multiple-test correction was applied using a local and tail area-based approach (Strimmer, 2008) and differences in phosphorylation levels cut at $\text{padj} < 0.00001$ and \log_2 fold > 5 . Gene ontology enrichment analysis was performed using STRING-DB (Szkłarczyk et al., 2023), with the Hochberg and Benjamini correction applied to estimate false discovery rates. For each condition, three biological replicates were done at each of three cell passages.

2.7. Western blot

Protein lysates were produced from HaCaT cells, both control and exposed to FLX (540 ng/l) and scratched as for protein microarrays. Cells were lysed in 2% SDS (Gilbert et al., 2024). Protein lysates were boiled with Laemmli sample buffer and proteins (20–50 μg) were resolved through 10% SDS-PAGE gels run at 120 V. Western transfer was done for 2 h at 100 V and proteins transferred to a nitro-cellulose membrane (ECL Hybond). Membranes were incubated at 4 °C overnight in 1% milk in TBST (w:v) containing 1:1000 dilutions of primary antibodies (MAB8934-SP and MAB1094-SP against GSK3B S9 phosphorylation and MSK1(RPS6KA5, S376)/MSK2(RPS6KA4, S360) phosphorylation, respectively, both from R&D Systems), as appropriate. Binding was detected using horseradish peroxidase (HRP)-conjugated goat anti-rabbit antibody (Dako #P0448, 1:5000 dilution), using Clarity™ ECL Western substrate (Bio-Rad) and imaged as previously described (Marsden et al., 2021a,b; Onwuli et al., 2019). Densitometry analysis was performed in ImageJ (Schneider et al., 2012) and protein band intensity was normalised to loading control bands.

2.8. Statistical analyses

T-tests (for binary comparisons) and ANOVA followed by Tukey post-hoc tests (for multiple comparisons) statistical analyses were performed where data were parametric. Protein microarray data were non-parametric and analysed by PERMANOVA using the Adonis function from the vegan (<https://CRAN.R-project.org/package=vegan>) R package (R 4.1.2) using RStudio.

3. Results

3.1. Exposure to ER-FLX concentrations enhances scratch closure in a wound healing keratinocyte model

To investigate any effects of FLX at ER concentrations on wound healing, we first used a keratinocyte cell line model. We exposed HaCaT cells to a wide range of ER-FLX concentrations (62.5–5400 ng/l) for 28–36 h. We routinely observed a dose-dependent increase in scratch closure starting from 125 ng/l FLX (Fig. 1A–B and Supplementary Fig. 1).

To better understand the mechanistic basis and the specificity of this observation, we treated cells with mitomycin C (an inhibitor of cell proliferation), with a second SSRI, and with 5-HT receptor blockers. Firstly, treatment with mitomycin C abrogated the effects of exposure to FLX (Fig. 1C and Supplementary Fig. 2), showing that the enhancement of scratch closure promoted by FLX was inhibited in the presence of cell proliferation inhibitors. We thus inferred that exposure of scratched HaCaT cells to FLX induced an increase in cell proliferation which, in turn, led to faster scratch closure. To test this hypothesis, we labelled proliferating cells in scratch assays with EdU. We observed a dose-response relationship between the concentration of FLX and the number of cells labelled by EdU (Fig. 1D). As a control, we repeated some of the EdU experiments in the presence of mitomycin C. As expected, the addition of mitomycin C abrogated the increase in EdU labelling observed with FLX (Supplementary Fig. 3).

Secondly, we tested another SSRI, sertraline, to explore the specificity of our findings. We incubated HaCaT cells with sertraline and performed scratch assays as before. Results mirrored those using FLX (Fig. 1E and Supplementary Fig. 5), and we observed enhanced scratch closure in the presence of ng/l concentrations of sertraline. Together, our observations strongly suggested that SSRIs promoted scratch closure through cell proliferation and we rationalised that the most likely mechanism was through altering 5-HT signalling. To test this hypothesis, we first used RNAseq to identify the main 5-HT receptors expressed in HaCaT cells and we found evidence for expression of 5-HTRs from the seven families (Supplementary Table 1). We then treated cells with ketanserin (an antagonist of 5-HTR_{2a} and 5-HTR_{2c} that has been previously used to investigate the role of 5-HT in wound healing, including in clinical trials) (Janssen et al., 1989; Lawrence et al., 1995; Nguyen et al., 2019; Sadiq et al., 2018). Ketanserin treatment reversed the effect of FLX on scratch closure (Fig. 1F), which clearly showed that the FLX-induced enhancement of scratch closure depended upon 5-HT signalling through 5-HTRs.

3.2. Exposure to ER-FLX activates transcriptomic networks associated with cell proliferation

We sought to understand the molecular mechanisms underlying the enhancement of cell proliferation and scratch closure when HaCaT cells were exposed to ER-FLX concentrations. Firstly, we performed a transcriptomics analysis of the effects of exposure. Given that increased cell proliferation was visible after 28–36 h exposure (Fig. 1), we reasoned that changes in gene expression may occur earlier than that. To test this hypothesis, we exposed scratched HaCaT cells to 540 ng/l FLX for 6 and 36 h, and analysed gene expression compared to control (not exposed) cells. A total of 21,403 (or 31,102) transcripts were sequenced in all (or at least one) samples at depths between 43 and 76 million reads per sample, with 94–97% mapped to exonic regions (NCBI's Gene Expression Omnibus (GEO)- accession number ([dataset] GSE268987).

We found 350 differentially expressed genes (DEGs) between control and exposed samples after 36 h (Fig. 2A and Supplementary Table 2). Gene Ontology (GO) term, Reactome and KEGG pathways enrichment analysis clearly identified altered respiration, mitochondrial metabolism, ribonucleoside/ribonucleotide metabolism, oxidative phosphorylation and thermogenesis in DEGs downregulated after 36 h of FLX exposure (Supplementary Figs. 6–8 and Supplementary Tables 3–5). In upregulated DEGs, we found GO terms related to cell proliferation and tissue morphogenesis (Supplementary Fig. 9). These findings were remarkable in the context of a modest number of DEGs (Fig. 2B), and support the specificity of our results. STRING analysis revealed close interactions among DEG products, with clusters of ribosomal and mitochondrial proteins (Supplementary Fig. 10). Taken together, the downregulation of transcriptomic networks associated with mitochondrial function and the upregulation of the expression of genes involved in cell proliferation are consistent with our previous data showing enhancement of cell proliferation by ER-FLX. Contrary to our expectations, the number of DEGs (Fig. 2C) and the enrichment in GO terms and pathways (Supplementary Table 6) were lower in HaCaT cells exposed to ER-FLX for 6 h only, with a just-significant GO term enrichment in glutathione transferase activity which may be indicative of an early mitochondrial metabolism switch.

3.3. Exposure to ER-FLX changes kinase phosphorylation profiles

Serotonin signalling is regulated by protein kinases and protein phosphorylation (Sahu et al., 2018). Having shown that the mechanism underlying the effects of ER-FLX on cells was through 5-HT signalling (Fig. 1F), we hypothesised that protein kinases, particularly those related to MAPK pathways, were differentially phosphorylated upon exposure. To test this hypothesis, we exposed scratched HaCaT cells to 540 ng/l FLX for 6 and 36 h and we profiled the levels of

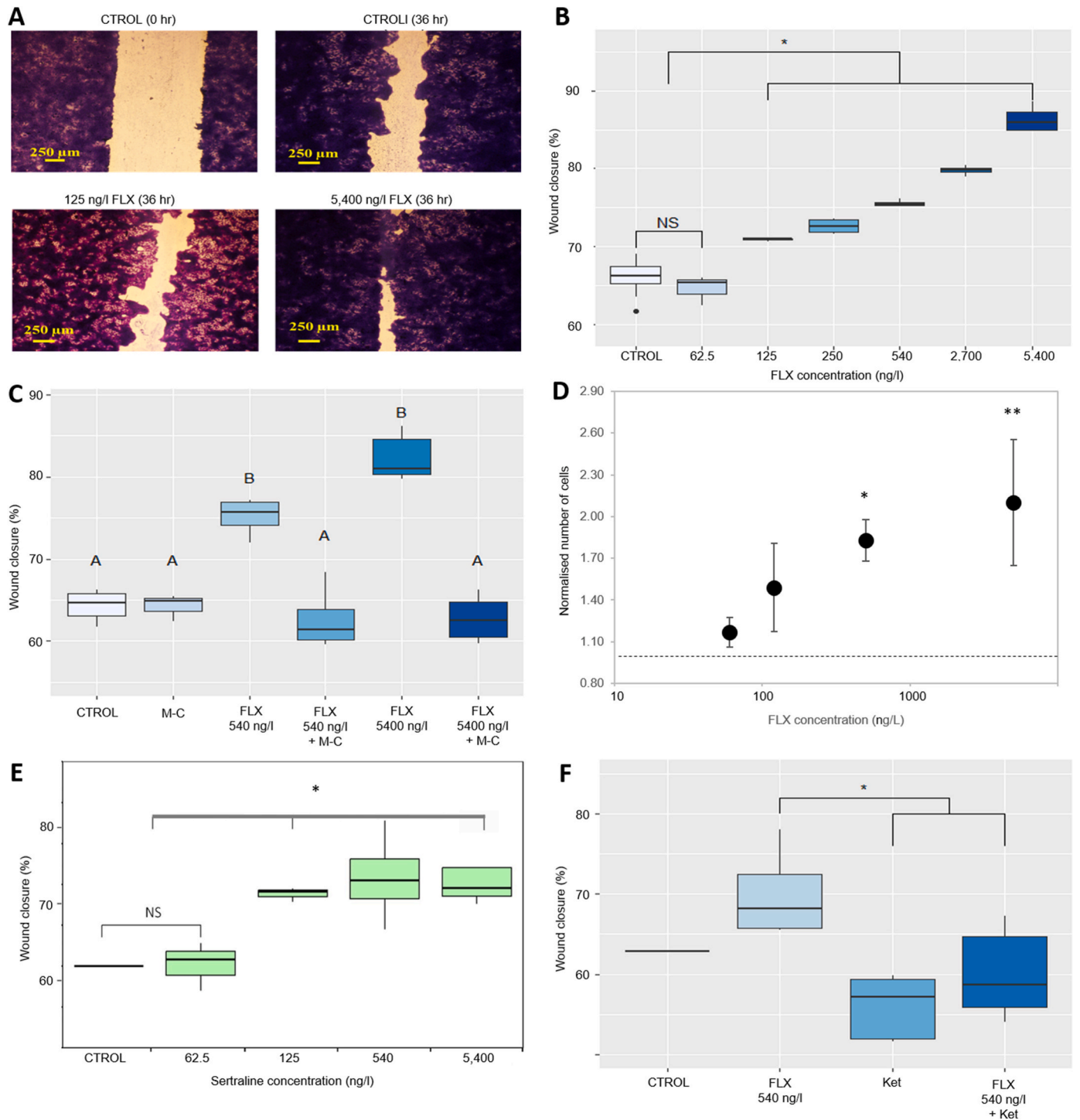


Fig. 1. A. Representative images of scratch assays in the presence of FLX, at the indicated concentrations, and visualised at the start of the experiment (0 h, top left) or after 36 h. Scratches at time 0 h were of a width of 1 ± 0.12 mm ($n = 4$). B. Dose-response dependence of scratch (wound) closure on FLX concentration. X axis not to scale. NS: non-significant. * $p < 0.05$ (0.003556 and 0.000019 for 125 and 250 ng/l, and < 0.00001 for 540, 2700 and 5400 ng/l each vs control). C. Treatment with mitomycin C (M-C) reversed the effect of FLX. Samples labelled as 'B' are significantly different ($p < 0.05$) to samples labelled as 'A'. D. Dose-response dependence of the number of proliferating cells, as judged by EdU labelling, on FLX concentration (in log scale). * $p = 0.01$, ** $p = 0.0023$ vs control (dotted line). E. Dose-response dependence of scratch (wound) closure on sertraline concentration. X axis not to scale. NS: non-significant. Significant p-values were as follows: sertraline 125, 540 and 5400 ng/l vs control: 0.045, 0.0072 and 0.006 respectively (labelled with *); sertraline 540 and 5400 ng/l vs sertraline 62.5 ng/l: 0.014 and 0.012, respectively. F. Treatment with ketanserin (Ket) reversed the effect of FLX on scratch (wound) closure. Significant p-values were as follows: $p = 0.000388$ (FLX vs Ket), 0.0031226 (FLX vs FLX + Ket).

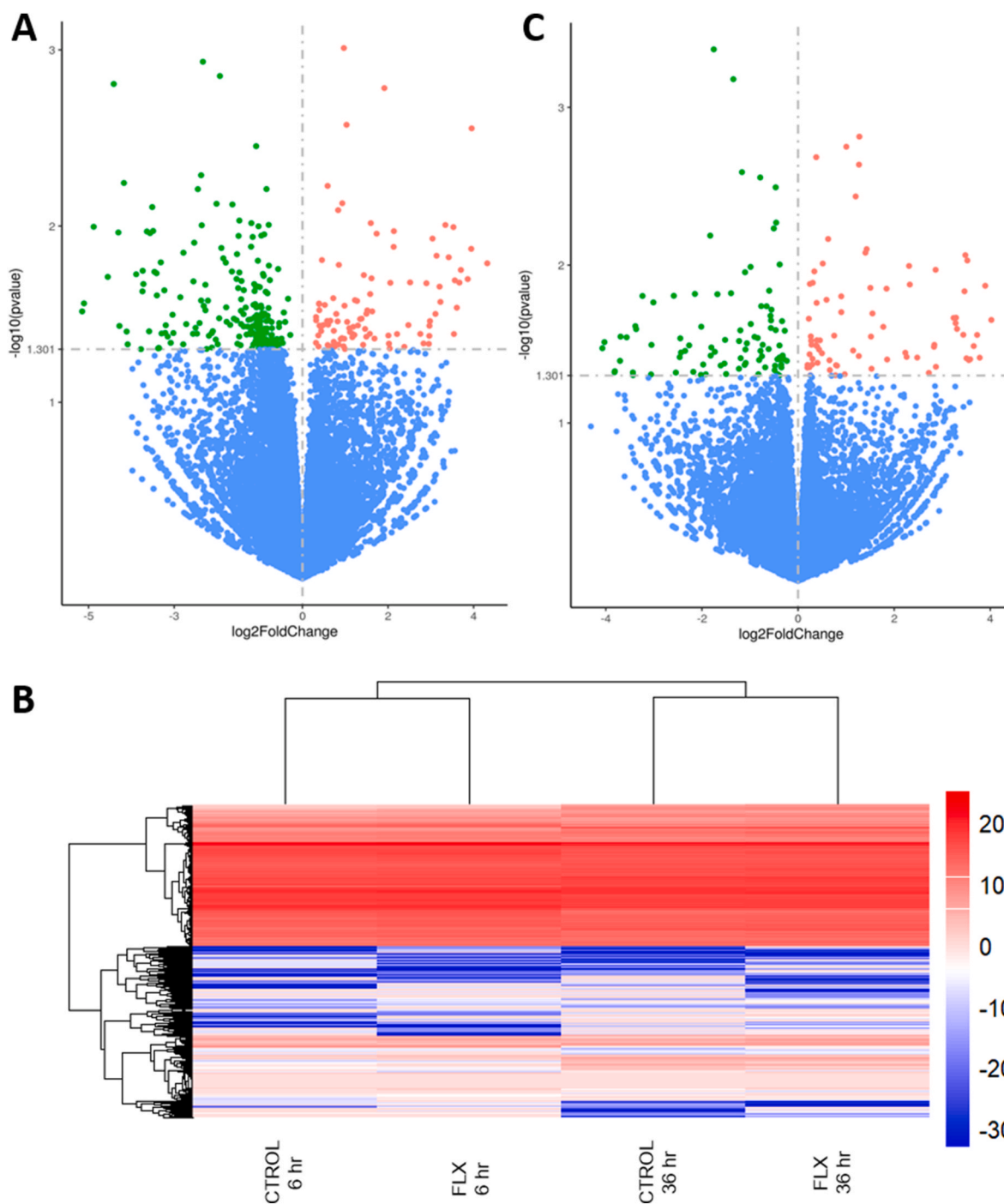


Fig. 2. A: Volcano plot illustrating 100 upregulated (in red) and 250 downregulated (in green) genes after 36 h exposure to 540 ng/l FLX. In blue, 26670 genes not differentially expressed. B: Heatmap comparing global gene expression (\log_2 gene counts, average of 4 replicates) in HaCaT cells treated with 540 ng/l for 6 and 36 h, and respective controls. C: Volcano plot illustrating 76 upregulated (in red) and 89 downregulated (in green) genes after 6 h exposure to 540 ng/l FLX. In blue, 25141 genes not differentially expressed. (For interpretation of the references to colour in this figure legend, the reader is referred to the Web version of this article.)

phosphorylation of 37 kinases at each endpoint using high-throughput protein microarrays. We found trends ($\text{padj} = 0.1$) toward reductions in the levels of phosphorylated glycogen-synthase kinase 3 (at least the β isoform, GSK3B) and the serine/threonine-protein kinase WNK1 after 6 h. After 36 h exposure, we found trends toward reduced phosphorylation of GSK3A/B, Proto-oncogene tyrosine-protein kinase (SRC) and Ribosomal protein S6 kinase alpha-4/-5 (RPS6KA4/RPS6KA5), while p70 S6 kinase (RPS6KB1) phosphorylation levels tended to increase (Fig. 3A–C). We validated a subset of these results using Western blot and we showed statistically significant reductions in the levels of

phosphorylation of GSK3B and RPS6KA5 (Fig. 3D–E).

Altered levels of phosphorylated kinases could be due to changes in kinase expression levels. To test this hypothesis, we analysed the levels of gene expression of GSK3A, GSK3B, SRC, WNK1, RPS6KA4/5 and p70 S6 kinase using our RNAseq dataset, and we found no statistically significant differences between control and exposed cells at either endpoint (6 or 36 h) (Supplementary Table 2).

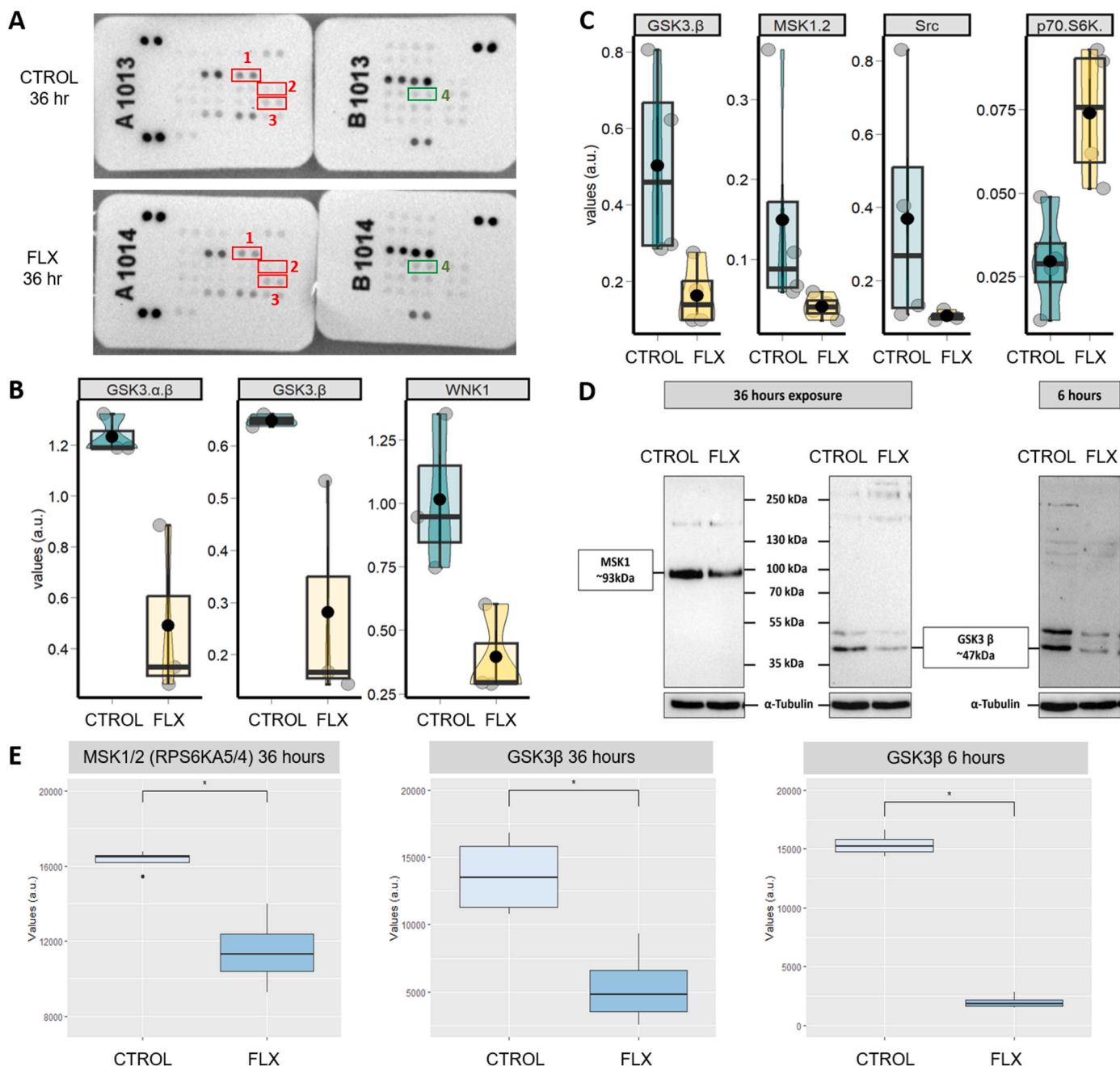


Fig. 3. **A:** Example of raw data from protein microarrays, showing reduced signal (in red) for phosphorylation of GSK3B (labelled as box 1) Ser9, RPS6KA5/4 (MSK1/2) Ser376/Ser360 (box 2), and SRC Tyr419 (box 3); and increased (in green) RPS6KB1 Thr421/Ser424 (box 4) phosphorylation. **B:** Box plot showing statistical analysis of 3 replicates after 6 h exposure to 540 ng/l FLX, compared to control. Left, GSK3 α or β isoforms (Ser21 or Ser9, respectively); centre, GSK3 β (Ser9); right, WNT1 (Thr60). All cases: padj = 0.1. **C:** Box plot showing statistical analysis of 4 replicates after 36 h exposure to 540 ng/l FLX, compared to control. From left to right, GSK3 β (Ser9); RPS6KA5/4 (MSK1 or 2, Ser376 or Ser360 respectively); SRC (Tyr419) and p70 S6 kinase (PR6KB1, Thr421/Ser424). All cases: padj = 0.1. **D:** Raw western blots showing reduced phosphorylation of RPS6KA5/4 (MSK1/2) and GSK3B in exposed samples (FLX) compared to controls, at the indicated exposure times. α -tubulin was used as loading control. **E:** Box plot showing statistical analysis of $n > 3$ Western blot replicates, * from left to right, $p = 0.0034675$ (MSK1/2), 0.0073869 (GSK3 β 36 h) and 0.0000005 (GSK3 β 6 h). (For interpretation of the references to colour in this figure legend, the reader is referred to the Web version of this article.)

3.4. Exposure to ER-FLX leads to 235 differentially phosphorylated proteins

Given the effects of exposure to ER-FLX on kinase phosphorylation profiles, we reasoned that changes in protein phosphorylation at the proteome level should follow. To test this hypothesis and to identify the target proteins undergoing differential phosphorylation in FLX-exposed cells, we performed phosphoproteomic analyses of HaCaT cells exposed

to 540 ng/l FLX. Based on our previous findings showing greater effects after 36 h than after 6 h of exposure at the transcriptomic and kinase phosphorylation levels, phosphoproteomics experiments were designed to identify phosphosites after 36 h exposure only. We found a total of 235 phosphopeptides that were differentially phosphorylated in exposed cells (Fig. 4A–B, Supplementary Table 7 and ProteomeXchange ([dataset] PXD052227) and MassIVE ([dataset] MSV000094745) (doi:10.25345/C54X54T49)).

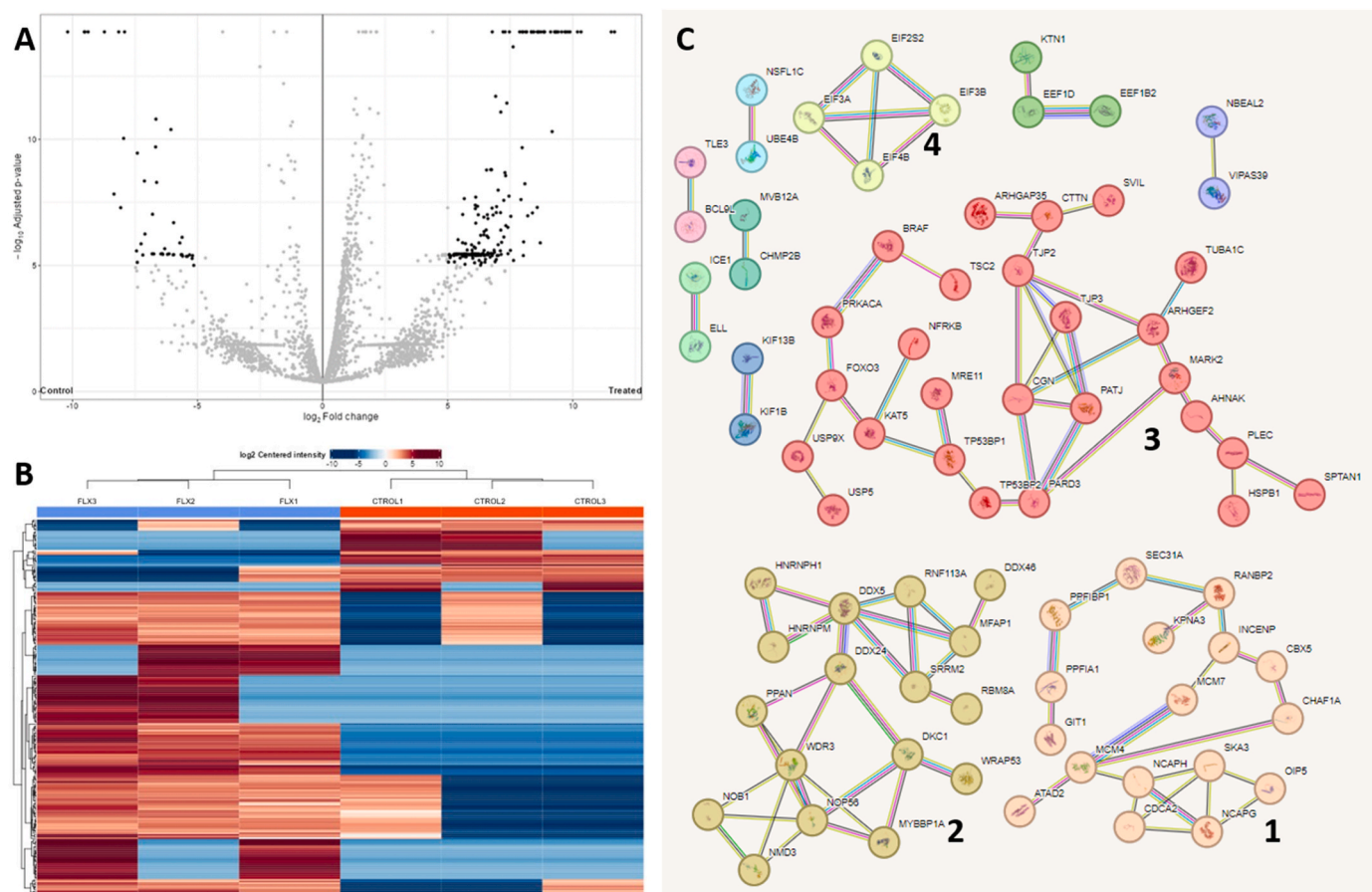


Fig. 4. A: Volcano plot illustrating 190 upregulated and 45 downregulated phosphosites after 36 h exposure to 540 ng/l FLX (black dots) at $p_{adj} < 0.00001$. B: Heatmap comparing phosphosites in HaCaT cells exposed to 540 ng/l for 36 h, versus controls. Three individual replicates are shown for control (on the right, CTRL1-3) and exposed (on the left, FLX1-3) samples. C: Clusters of protein-protein interactions within proteins with upregulated phosphorylation levels upon exposure. For clarity, only the highest confidence interactions are shown (STRING interaction score > 0.9). Cluster 1: DNA repair, cell signalling and structures associated with epithelial cell fate cluster. Cluster 2: ribonucleoproteins cluster. Cluster 3: chromosome organisation cluster. Cluster 4: elongation initiation factor cluster. No enrichment in GO terms or pathways was found within proteins with downregulated phosphorylation levels.

Within the proteins hyperphosphorylated in treated cells, we found an enrichment in GO terms and pathways related to cell cycle and division, cellular and chromosome organisation, and mRNA and protein biosynthesis, among others (Supplementary Table 7). Proteins clustered into several, well-defined protein-protein interactions networks around chromosome organisation, ribonucleoproteins, elongation initiation factors, and DNA repair, cell signalling and structures associated with epithelial cell fate (Fig. 4C). Taken together, these results are consistent with our earlier observation that ER-FLX promotes HaCaT cell proliferation.

3.5. FLX promotes wound closure in an *ex vivo* model of wound healing using human skin biopsies

To investigate the relevance of our results to human skin wound healing, we exposed skin biopsies to FLX for 48 h *ex vivo* (clinical data in Supplementary Table 8). These experiments used higher FLX concentrations (2.5 and 5 $\mu\text{g/l}$), which have previously been used as upper limits for ER-FLX levels (Correia et al., 2022; Dziejewczynski et al., 2016; Guler & Ford, 2010; Miranda et al., 2023; Weinberger & Klaper, 2014).

We observed a statistically significant enhancement of wound closure in skin biopsies exposed to 2.5 and 5 $\mu\text{g/l}$ FLX, compared to control biopsies (Fig. 5A–B). Of note, the mechanistic basis underlying this observation must be augmented 5-HT signalling, because wound closure enhancement was reversed in the presence of the 5-HT antagonist ketanserin (Fig. 5C). These data are in accordance with our

findings using a cell line model and underscore the relevance of our results in the human wound microenvironment.

4. Discussion

Using several models of wound healing, we have shown that exposure to ER-FLX significantly enhances wound closure in HaCaT cells and human skin *ex vivo*. We used relevant FLX concentrations that are widely acknowledged as representative of ‘real world’, environmental settings, and report effects on wound healing from SSRI concentrations starting at 125 ng/l, which are well accepted as ER (De Castro-Català et al., 2017; De Lange et al., 2009; Painter et al., 2009; Woodman et al., 2016). We have dissected the mechanisms underlying these observations and shown that ER-FLX promotes cell proliferation through the 5-HT signalling pathway.

Chronic wounds present a complex, costly and challenging medical concern (Wilkinson & Hardman, 2020). These wounds, persisting for an extended period (> 12 weeks), are typically due to impaired or stalled wound healing mechanisms, which in turn can be due to underlying conditions such as diabetes or vascular disease. Previous clinical trials have targeted 5-HT signalling in wounds using ketanserin, with limited success (Janssen et al., 1989; Lawrence et al., 1995). There have also been recent attempts at investigating and developing novel treatment strategies based on repurposing FLX as a wound healing drug in various forms. The evidence we present here strongly indicates that the concentrations of FLX needed for an improvement in wound healing are

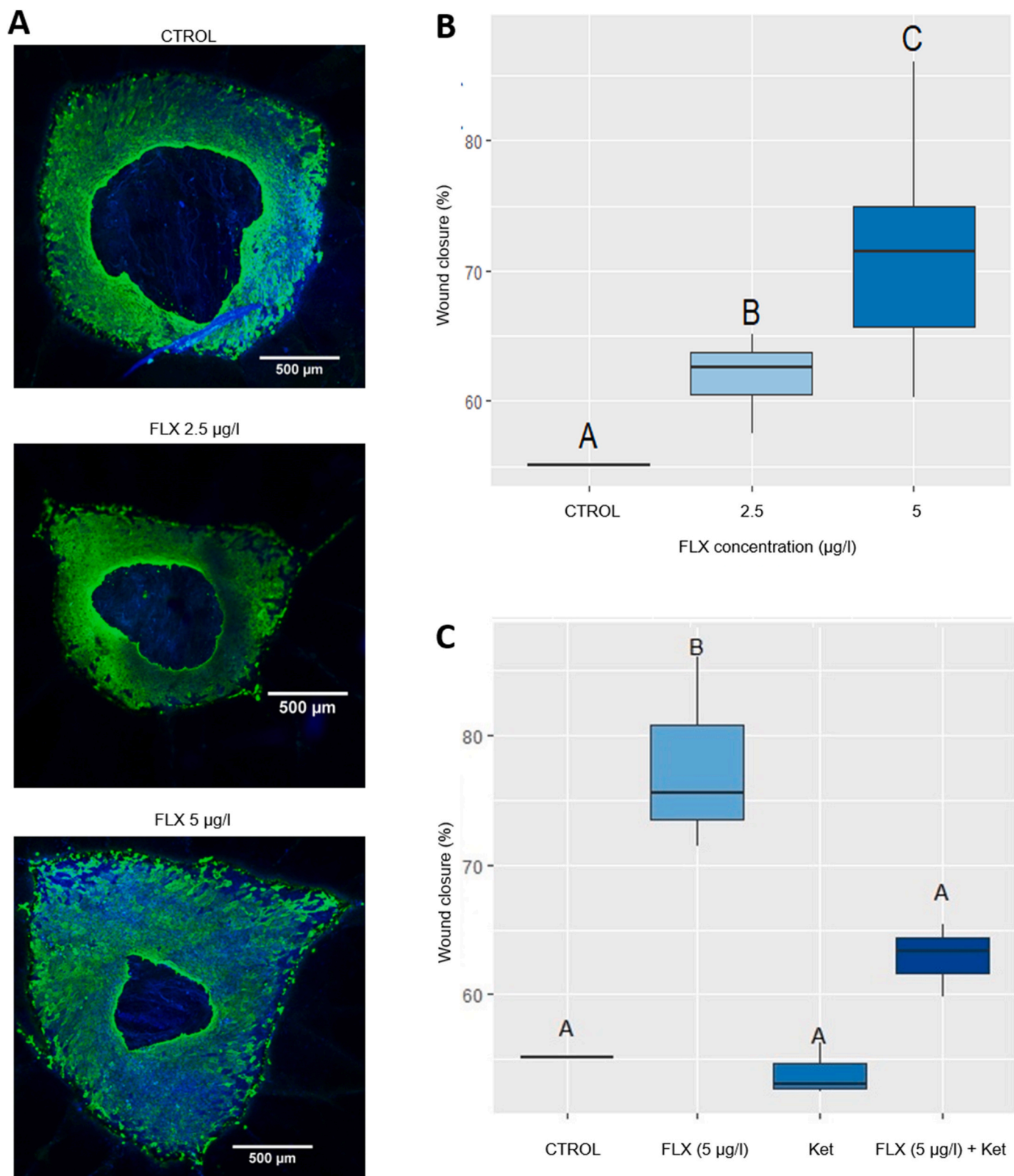


Fig. 5. A. Representative images (n = 4) of wound healing assays in the presence of FLX, at the indicated concentrations, and visualised after 48 h. In green, keratin 14; in blue, DAPI. Scale bar: 500 µm. B. Dose-response dependence of wound closure on FLX concentration. Samples labelled as 'B' and 'C' are significantly different between each other and also when compared to control, labelled 'A' (p = 0.0133656 and 0.0000003, respectively). C. Treatment with ketanserin (Ket) reverses the effect of FLX on wound closure. Samples labelled as 'B' are significantly different to samples labelled 'A', p = 0.009078 between FLX and FLX + Ket samples. (For interpretation of the references to colour in this figure legend, the reader is referred to the Web version of this article.)

much lower than previously thought, which can reduce drug loads and any side-effects of treatment in a clinical trial setting. A more intriguing medical implication of our work is the possibility that chronic exposure to ER-FLX leads to uncontrolled skin cell proliferation, a hallmark of cancer (Hanahan & Weinberg, 2011). Our RNAseq results support the notion that cells exposed to ER-FLX could switch to a proliferative metabolic state reminiscent of the Warburg effect (that is, decreased aerobic metabolism and increased glycolysis) (Antico Arciuch et al., 2012; Chandel, 2021). Clinically relevant doses of FLX have been shown to increase glycolysis (Pan et al., 2022) and the role of 5-HT signalling in controlling cell fate, including the proliferation of keratinocytes and fibroblasts, supports this line of thinking (Kim et al., 2018; Macdonald et al., 1958; Wang et al., 2014; Welsh et al., 2004). Indeed, exposure to (non-ER) FLX specifically increases the proliferation of brain cells (Imoto et al., 2015; Sousa-Ferreira et al., 2014), and breast cancer cells (Ballou et al., 2018; Brandes et al., 1992). Our observation that ER-FLX promotes wound healing will help us, first, better understand the risks (or potential benefits) to human health of the presence of SSRI in the environment and, second, justify efforts towards exploring the potential for behavioural changes at the system level that reduce the use of antidepressants altogether. The general public view on SSRIs is highly variable, on the one hand, there is a growing awareness and acceptance of mental health issues in societies. On the other hand, some criticise SSRIs for the treatment of mental disorders as 'quick fixes' for more complex issues (Golder et al., 2023). There are trends towards reducing oversubscription of antidepressants through green social prescribing schemes (Bray et al., 2022), which would reduce SSRI concentrations in environmental systems.

Our work also sheds light on previous, sometimes contradictory evidence on the role of 5-HT in wound healing. Serotonin is known to be part of various wound healing pathways. During the inflammatory phase, local 5-HT concentration is increased, as is expression of 5-HT receptors in B and T lymphocytes (Alstergren et al., 1999; Zhang et al., 2001). Proinflammatory cytokines such as IL-1b or Interferon-c upregulate the 5-HT transporter SERT (Mossner et al., 2001), and lymphocytes are recruited into the inflammatory focus through 5-HT signalling (Laberge et al., 1996), all pointing towards a role of 5-HT signalling in this phase. Serotonin also induces fibroblast proliferation and adhesion by upregulating the secretion of fibroblast growth factor-2 (FGF-2) (Seuwen et al., 1988). These mechanisms are relevant in our *ex vivo* model of wound healing using clinical biopsies, which recapitulates the wound microenvironment. Clinically, one of the most common tools to regulate 5-HT signalling in tissues (that is, the brain in the context of clinical depression) is through SSRIs, and SSRIs have also been used in previous research to investigate the effects of 5-HT in wound healing. For example, Yuksel et al. injected paroxetine in rats (both control and diabetic models) every day for 14 days and made excision wounds on their skin (Yuksel et al., 2014). The number of fibroblasts in the wound was significantly higher for treated rats compared with the saline-administered rats; but only in control and not in diabetic rats. Complete epithelisation was achieved only for paroxetine-administered and control (but not diabetic) rats (Yuksel et al., 2014). Fibroblasts and re-epithelisation play an important role in the proliferative phase of wound healing and this study showed that systemic treatment with paroxetine enhanced cutaneous wound healing *in vivo*, at least of non-diabetic rat skin. An analogous study investigated stressed rats (chronic social stress, that is, 24 h of isolation followed by 24 h of crowding) treated systemically with FLX for 14 days (1 mg/kg) (Farahani et al., 2007). FLX treatment increased wound healing rate by 68% and 31% for stressed and non-stressed rats, respectively. The authors hypothesised that this improvement in wound healing after treatment could be explained by FLX-induced increases in the level of IL-1 (Kubera et al., 2000), a cytokine that plays a significant role in the inflammatory phase of wound healing (Hu et al., 2010). Despite using much lower FLX concentrations, our results generally agree with the view that SSRI enhance wound healing, a conclusion that is supported

by both our cell line and our clinical biopsies models. Previous studies on the effects of FLX on wound healing have used cell lines and animal models. In contrast, here we chose to use human samples to maximise physiological and clinical relevance and impact. Although the study cohort was small and heterogenous (Supplementary Table 8), our results clearly showed increased wound healing after 48 h exposure. At the molecular level, we showed that the main mechanism underlying the effects of FLX, at least at ER concentrations and in HaCaT cells, was increased cell proliferation. This compares to cell migration which was proposed by Nguyen et al. (2019) when using Normal Human Epidermal Keratinocytes (NHEK). Yoon et al., and Nguyen et al., used FLX at concentrations up to 8 orders of magnitude higher than those in this work (Nguyen et al., 2019; Yoon et al., 2021) and it is possible that other mechanisms, including increased cell migration, may become prominent at these higher doses.

The above reports that non-diabetic and stressed rats 'benefit' more from treatment with SSRI underscore the complex interactions between underlying pathologies and wound healing. Our study investigated human skin from donors undergoing elective surgery and further research is warranted to investigate the effects of ER-FLX on skin from e. g., people with chronic wounds. We also acknowledge that we exposed cells and biopsies to FLX in isolation, while environmental matrices are likely to be much more complex. Based on literature, we had identified mitogen-activated protein kinases (MAPK) as master regulators of 5-HT signalling (Hsiung et al., 2005; Nebigil et al., 2003; Sahu et al., 2018) and we expected changes in the levels of phosphorylation of ERK1/2 (MAPK3/1), the T202/Y204 and T185/Y187 phosphorylation sites of which were included in our protein microarrays. While this was not the case in our hands, perhaps due to the transient nature of ERK1/2 phosphorylation, we did identify changes in the phosphorylation of RPS6KA4/5, mitogen- and stress-activated protein kinases that are activated by ERK2 and phosphorylate the MAPK mediator CREB (Deak et al., 1998). The relevance of MAPK signalling is also supported by our phosphoproteomics results, which showed hyperphosphorylation of MAPK kinases MAP3K3, MAP3K4 and MAP4K5 in exposed cells (Supplementary Table 7). The observation that exposure to ER-FLX regulates GSK3, SRC and p70 S6 kinases is consistent with previous reports, which have made direct links between 5-HT signalling and GSK3A and B (Polter et al., 2012), SRC (Zavaritskaya et al., 2017), and p70 S6 kinase (Zamani & Qu, 2012). Of note, GSK3A/B, RPS6KA4/5, SRC and p70 S6 kinase are all interconnected through ERK1/2 (Supplementary Fig. 11) and a golden thread of cell metabolism, cell proliferation, cell growth and cell cycle progression (Vindis et al., 2003; Zheng et al., 2009). Taken together, our observation that exposure to ER-FLX concentrations changed the profile of phosphorylation of several protein kinases involved in cell fate decisions was consistent with the identification of differentially phosphorylated proteins in cells exposed to FLX and with the GO terms and biochemical pathways enriched in these differentially phosphorylated proteins.

Our work is the first to investigate the effects of FLX (at any concentration) on wound healing using -omics technologies, including transcriptomics and phosphoproteomics, and we took this systems biology approach due to the complexities of interlinked 5-HT signalling pathways (Sahu et al., 2018). The reduced number of DEGs after 6 h exposure was unexpected, but the enrichment in glutathione transferase activity GO terms at this endpoint was consistent with recent reports linking FLX to oxidative stress (Correia et al., 2023; Pinto et al., 2024). There was very little overlap between DEGs and differentially phosphorylated proteins measured after 36 h of exposure (Supplementary Tables 2 and 7), but both RNAseq and phosphoproteomics results strongly supported the conclusion that ER-FLX enhanced cell proliferation at the 36 h endpoint. This means that exposure to ER-FLX caused changes at both the gene expression and the protein phosphorylation levels that independently promoted cell proliferation. This is congruent with our phenotypic observation of improved wound healing in cell models and human biopsies.

5. Conclusion

We have shown that exposure to ER-FLX concentrations promotes scratch closure and wound healing in keratinocytes and clinical biopsies, respectively. This effect was dose- and also serotonin-dependent, because it was reversed by a 5-HT receptor blocker. Mechanistically, exposure led to hundreds of DEGs and differentially phosphorylated proteins, the latter including through modulation of MAPK-related kinases. Collectively, these changes at the gene and protein levels were associated with increased cell proliferation and an inhibitor of cell proliferation reversed the effect of ER-FLX. These results pave the way to environmental and clinical research into the effects of environmental SSRI on human skin wound healing. Our results also open new avenues for transdisciplinary research around the effects of ER-FLX on aquatic animals. Non-surprisingly given the clinical applications of SSRI, over the past 25 years research has focused on the impact of ER-FLX on *behaviour* (widely understood) of a range of aquatic species, often with modest results. Recent research has begun to uncover other impacts (Correia et al., 2023), e.g., on oxidative stress and fatty acid profiles (Pinto et al., 2024) and on ecosystems (Michelangeli et al., 2024), but we are not aware of any study investigating wound healing impacts of exposure. Our results justify a transition from the study of behavioural effects of ER-FLX in fish to the investigation of effects of exposure on wound healing in aquatic and terrestrial animals, including direct impacts on human health. We argue that there is an urgent need to develop models that can inform risk assessment and regulatory decision making (Hollert & Keiter, 2015; Osaki et al., 2018).

Funding

QRB acknowledges a 'Happy Chemical' PhD studentship funded by the University of Hull. BGM would also like to express her gratitude to the Spanish Ministry of Science, Innovation and Universities for the FPI predoctoral contract PRE2019-089339 and to the University of Cantabria for the predoctoral mobility grant Erasmus+ n° 2021-1-ES01-KA131-HED-000005117. The York Centre of Excellence in Mass Spectrometry was created thanks to a major capital investment through Science City York, supported by Yorkshire Forward with funds from the Northern Way Initiative, and subsequent support from EPSRC (EP/K039660/1; EP/M028127/1).

CRediT authorship contribution statement

Quentin Rodriguez-Barucg: Writing – review & editing, Writing – original draft, Visualization, Validation, Software, Methodology, Investigation, Formal analysis, Data curation. **Angel A. Garcia:** Writing – review & editing, Supervision, Methodology, Investigation, Formal analysis, Data curation. **Belen Garcia-Merino:** Writing – review & editing, Writing – original draft, Methodology, Investigation, Funding acquisition, Formal analysis, Data curation. **Tomilayo Akinmola:** Writing – review & editing, Methodology, Investigation, Formal analysis, Data curation. **Temisanren Okotie-Eboh:** Writing – review & editing, Methodology, Investigation, Formal analysis, Data curation. **Thomas Francis:** Writing – review & editing, Methodology. **Eugenio Bringas:** Writing – review & editing, Resources, Investigation, Formal analysis. **Inmaculada Ortiz:** Supervision, Resources, Investigation, Formal analysis. **Mark A. Wade:** Writing – review & editing, Supervision, Resources, Methodology, Investigation. **Adam Dowle:** Writing – review & editing, Visualization, Validation, Software, Resources, Methodology, Investigation, Funding acquisition, Formal analysis, Data curation. **Domino A. Joyce:** Writing – review & editing, Validation, Supervision, Resources, Project administration, Methodology, Investigation, Funding acquisition, Formal analysis, Data curation, Conceptualization. **Matthew J. Hardman:** Writing – review & editing, Visualization, Validation, Supervision, Software, Resources, Project administration, Methodology, Investigation, Funding acquisition,

Formal analysis, Data curation. **Holly N. Wilkinson:** Writing – review & editing, Visualization, Validation, Supervision, Software, Resources, Project administration, Methodology, Investigation, Funding acquisition, Formal analysis, Data curation. **Pedro Beltran-Alvarez:** Writing – review & editing, Writing – original draft, Visualization, Validation, Supervision, Software, Resources, Project administration, Methodology, Investigation, Funding acquisition, Formal analysis, Data curation, Conceptualization.

Declaration of competing interest

The authors declare that they have no known competing financial interests or personal relationships that could have appeared to influence the work reported in this paper.

Data availability

Transcriptomics and proteomics data have been uploaded to relevant databases, please see access references in the manuscript

Acknowledgements

We thank previous students in the Beltran-Alvarez, Wilkinson and Hardman groups, including Inimbom Akpan, Abimbola Bankole and Amber R. Stafford for their contributions and for training.

Appendix A. Supplementary data

Supplementary data to this article can be found online at <https://doi.org/10.1016/j.envpol.2024.124952>.

References

- Alstergren, P., Ernberg, M., Kopp, S., Lundeberg, T., Theodorsson, E., 1999. TMJ pain in relation to circulating neuropeptide Y, serotonin, and interleukin-1 beta in rheumatoid arthritis. *J. Orofac. Pain* 13 (1), 49–55. <https://www.ncbi.nlm.nih.gov/pubmed/10425968>.
- Antico Arciuch, V.G., Elguero, M.E., Poderoso, J.J., Carreras, M.C., 2012. Mitochondrial regulation of cell cycle and proliferation. *Antioxidants Redox Signal.* 16 (10), 1150–1180. <https://doi.org/10.1089/ars.2011.4085>.
- Ballou, Y., Rivas, A., Belmont, A., Patel, L., Amaya, C.N., Lipson, S., Khayou, T., Dickerson, E.B., Nahleh, Z., Bryan, B.A., 2018. 5-HT serotonin receptors modulate mitogenic signaling and impact tumor cell viability. *Mol Clin Oncol* 9 (3), 243–254. <https://doi.org/10.3892/mco.2018.1681>.
- Barry, A., Samuel, S.F., Hosni, I., Moursi, A., Feugere, L., Sennett, C.J., Deepak, S., Achawal, S., Rajaraman, C., Iles, A., Wollenberg Valero, K.C., Scott, I.S., Green, V., Stead, L.F., Greenman, J., Wade, M.A., Beltran-Alvarez, P., 2023. Investigating the effects of arginine methylation inhibitors on microdissected brain tumour biopsies maintained in a miniaturised perfusion system. *Lab Chip* 23 (11), 2664–2682. <https://doi.org/10.1039/d3lc00204g>.
- Batt, A.L., Kostich, M.S., Lazorchak, J.M., 2008. Analysis of ecologically relevant pharmaceuticals in wastewater and surface water using selective solid-phase extraction and UPLC-MS/MS. *Anal. Chem.* 80 (13), 5021–5030. <https://doi.org/10.1021/ac800066n>.
- Bertram, M.G., Ecker, T.E., Wong, B.B.M., O'Bryan, M.K., Baumgartner, J.B., Martin, J. M., Saaristo, M., 2018. The antidepressant fluoxetine alters mechanisms of pre- and post-copulatory sexual selection in the eastern mosquitofish (*Gambusia holbrooki*). *Environ. Pollut.* 238, 238–247. <https://doi.org/10.1016/j.envpol.2018.03.006>.
- Blair, B.D., Crago, J.P., Hedman, C.J., Klaper, R.D., 2013. Pharmaceuticals and personal care products found in the Great Lakes above concentrations of environmental concern. *Chemosphere* 93 (9), 2116–2123. <https://doi.org/10.1016/j.chemosphere.2013.07.057>.
- Bossus, M.C., Guler, Y.Z., Short, S.J., Morrison, E.R., Ford, A.T., 2014. Behavioural and transcriptional changes in the amphipod *Echinogammarus marinus* exposed to two antidepressants, fluoxetine and sertraline. *Aquat. Toxicol.* 151, 46–56. <https://doi.org/10.1016/j.aquatox.2013.11.025>.
- Brandes, L.J., Arron, R.J., Bogdanovic, R.P., Tong, J., Zaborniak, C.L., Hogg, G.R., Warrington, R.C., Fang, W., LaBella, F.S., 1992. Stimulation of malignant growth in rodents by antidepressant drugs at clinically relevant doses. *Cancer Res.* 52 (13), 3796–3800. <https://www.ncbi.nlm.nih.gov/pubmed/1617649>.
- Bray, I., Reece, R., Sinnott, D., Martin, F., Hayward, R., 2022. Exploring the role of exposure to green and blue spaces in preventing anxiety and depression among young people aged 14–24 years living in urban settings: a systematic review and conceptual framework. *Environ. Res.* 214 (Pt 4), 114081 <https://doi.org/10.1016/j.envres.2022.114081>.

- Brooks, B.W., Chambliss, C.K., Stanley, J.K., Ramirez, A., Banks, K.E., Johnson, R.D., Lewis, R.J., 2005. Determination of select antidepressants in fish from an effluent-dominated stream. *Environ. Toxicol. Chem.* 24 (2), 464–469. <https://doi.org/10.1089/04-081r.1>.
- Chandel, N.S., 2021. Metabolism of proliferating cells. *Cold Spring Harbor Perspect. Biol.* 13 (10) <https://doi.org/10.1101/cshperspect.a040618>.
- Cizmas, L., Sharma, V.K., Gray, C.M., McDonald, T.J., 2015. Pharmaceuticals and personal care products in waters: occurrence, toxicity, and risk. *Environ. Chem. Lett.* 13 (4), 381–394. <https://doi.org/10.1007/s10311-015-0524-4>.
- Coleman, J.A., Green, E.M., Gouaux, E., 2016. X-ray structures and mechanism of the human serotonin transporter. *Nature* 532 (7599), 334–339. <https://doi.org/10.1038/nature17629>.
- Correia, D., Domingues, I., Faria, M., Oliveira, M., 2022. Chronic effects of fluoxetine on: a biochemical and behavioral perspective. *Applied Sciences-Basel* 12 (4). <https://doi.org/10.3390/app12042256>.
- Correia, D., Domingues, I., Faria, M., Oliveira, M., 2023. Effects of fluoxetine on fish: what do we know and where should we focus our efforts in the future? *Sci. Total Environ.* 857 (Pt 2), 159486. <https://doi.org/10.1016/j.scitotenv.2022.159486>.
- Curytek, K., Maes, M., Kubera, M., 2021. Immune-regulatory and molecular effects of antidepressants on the inflamed human keratinocyte HaCaT cell line. *Neurotox. Res.* 39 (4), 1211–1226. <https://doi.org/10.1007/s12640-021-00367-5>.
- Daughton, C.G., Ternes, T.A., 1999. Pharmaceuticals and personal care products in the environment: agents of subtle change? *Environ. Health Perspect.* 107 (Suppl. 6), 907–938. <https://doi.org/10.1289/ehp.99107s6907>.
- De Castro-Catala, N., Muñoz, I., Riera, J.L., Ford, A.T., 2017. Evidence of low dose effects of the antidepressant fluoxetine and the fungicide prochloraz on the behavior of the keystone freshwater invertebrate *Gammarus pulex*. *Environ. Pollut.* 231 (Pt 1), 406–414. <https://doi.org/10.1016/j.envpol.2017.07.088>.
- De Castro-Catala, N., Muñoz, I., Riera, J.L., Ford, A.T., 2017. Evidence of low dose effects of the antidepressant fluoxetine and the fungicide prochloraz on the behavior of the keystone freshwater invertebrate. *Environ. Pollut.* 231, 406–414. <https://doi.org/10.1016/j.envpol.2017.07.088>.
- De Lange, H.J., Peeters, E.T.H.M., Lüring, M., 2009. Changes in ventilation and locomotion of (Crustacea, Amphipoda) in response to low concentrations of pharmaceuticals. *Human and Ecological Risk Assessment* 15 (1), 111–120. <https://doi.org/10.1080/10807030802615584>.
- Deak, M., Clifton, A.D., Lucoq, L.M., Alessi, D.R., 1998. Mitogen- and stress-activated protein kinase-1 (MSK1) is directly activated by MAPK and SAPK2/p38, and may mediate activation of CREB. *EMBO J.* 17 (15), 4426–4441. <https://doi.org/10.1093/emboj/17.15.4426>.
- Dziewieczynski, T.L., Campbell, B.A., Kane, J.L., 2016. Dose-dependent fluoxetine effects on boldness in male Siamese fighting fish. *J. Exp. Biol.* 219 (Pt 6), 797–804. <https://doi.org/10.1242/jeb.132761>.
- Edinoff, A.N., Akuly, H.A., Hanna, T.A., Ochoa, C.O., Patti, S.J., Ghaffar, Y.A., Kaye, A.D., Viswanath, O., Urits, I., Boyer, A.G., Cornett, E.M., Kaye, A.M., 2021. Selective serotonin reuptake inhibitors and adverse effects: a narrative review. *Neurol. Int.* 13 (3), 387–401. <https://doi.org/10.3390/neurolint13030038>.
- Farahani, R.M., Sadr, K., Rad, J.S., Mesgari, M., 2007. Fluoxetine enhances cutaneous wound healing in chronically stressed Wistar rats. *Adv. Skin Wound Care* 20 (3), 157–165. <https://doi.org/10.1097/01.ASW.0000262710.59293.6b>.
- Feugere, L., Bates, A., Emagbetere, T., Chapman, E., Malcolm, L., Bulmer, K., Hardege, J., Beltran-Alvarez, P., Valero, K.C.W., 2022. Heat induces multi-omic and phenotypic stress propagation in zebrafish embryos. *bioRxiv* 2022. <https://doi.org/10.1101/2022.09.15.508176>, 2009.2015.508176.
- Ford, A.T., Fong, P.P., 2016. The effects of antidepressants appear to be rapid and at environmentally relevant concentrations. *Environ. Toxicol. Chem.* 35 (4), 794–798. <https://doi.org/10.1002/etc.3087>.
- Gilbert, E., Zagar, A., Lopez-Darias, M., Megia-Palma, R., Lister, K.A., Jones, M.D., Carretero, M.A., Seren, N., Beltran-Alvarez, P., Valero, K.C.W., 2024. Environmental factors influence cross-talk between a heat shock protein and an oxidative stress protein modification in the lizard *Gallotia galloti*. *PLoS One* 19 (3), e0300111. <https://doi.org/10.1371/journal.pone.0300111>.
- Golder, S., Medaglio, D., O'Connor, K., Hennessy, S., Gross, R., Gonzalez Hernandez, G., 2023. Reasons for discontinuation or change of selective serotonin reuptake inhibitors in online drug reviews. *JAMA Netw. Open* 6 (7), e2323746. <https://doi.org/10.1001/jamanetworkopen.2023.23746>.
- Gosmann, N.P., Costa, M.A., Jaeger, M.B., Motta, L.S., Frozi, J., Spanemberg, L., Manfro, G.G., Cuijpers, P., Pine, D.S., Salum, G.A., 2021. Selective serotonin reuptake inhibitors, and serotonin and norepinephrine reuptake inhibitors for anxiety, obsessive-compulsive, and stress disorders: a 3-level network meta-analysis. *PLoS Med.* 18 (6), e1003664. <https://doi.org/10.1371/journal.pmed.1003664>.
- Gros, M., Petrovic, M., Barcelo, D., 2009. Tracing pharmaceutical residues of different therapeutic classes in environmental waters by using liquid chromatography/quadrupole-linear ion trap mass spectrometry and automated library searching. *Anal. Chem.* 81 (3), 898–912. <https://doi.org/10.1021/ac801358e>.
- Grzesiuk, M., Gryglewicz, E., Bentkowski, P., Pijanowska, J., 2023. Impact of fluoxetine on herbivorous zooplankton and planktivorous fish. *Environ. Toxicol. Chem.* 42 (2), 385–392. <https://doi.org/10.1002/etc.5525>.
- Guler, Y., Ford, A.T., 2010. Anti-depressants make amphipods see the light. *Aquat. Toxicol.* 99 (3), 397–404. <https://doi.org/10.1016/j.aquatox.2010.05.019>.
- Hanahan, D., Weinberg, R.A., 2011. Hallmarks of cancer: the next generation. *Cell* 144 (5), 646–674. <https://doi.org/10.1016/j.cell.2011.02.013>.
- Haub, S., Ritze, Y., Bergheim, I., Pabst, O., Gershon, M.D., Bischoff, S.C., 2010. Enhancement of intestinal inflammation in mice lacking interleukin 10 by deletion of the serotonin reuptake transporter. *Neuro Gastroenterol. Motil.* 22 (7), 826. <https://doi.org/10.1111/j.1365-2982.2010.01479.x>, 34, e229.
- Hollert, H., Keiter, S.H., 2015. Danio rerio as a model in aquatic toxicology and sediment research. *Environ. Sci. Pollut. Res. Int.* 22 (21), 16243–16246. <https://doi.org/10.1007/s11356-015-5362-1>.
- Hsiung, S.C., Tamir, H., Franke, T.F., Liu, K.P., 2005. Roles of extracellular signal-regulated kinase and Akt signaling in coordinating nuclear transcription factor-kappaB-dependent cell survival after serotonin 1A receptor activation. *J. Neurochem.* 95 (6), 1653–1666. <https://doi.org/10.1111/j.1471-4159.2005.03496.x>.
- Hu, Y.J., Liang, D.Y., Li, X.Q., Liu, H.H., Zhang, X., Zheng, M., Dill, D., Shi, X.Y., Qiao, Y. L., Yeomans, D., Carvalho, B., Angst, M.S., Clark, J.D., Peltz, G., 2010. The role of interleukin-1 in wound biology. Part II: in vivo and human translational studies. *Anesth. Analg.* 111 (6), 1534–1542. <https://doi.org/10.1213/ANE.0b013e3181f691eb>.
- Imoto, Y., Kira, T., Sukeno, M., Nishitani, N., Nagayasu, K., Nakagawa, T., Kaneko, S., Kobayashi, K., Segi-Nishida, E., 2015. Role of the 5-HT4 receptor in chronic fluoxetine treatment-induced neurogenic activity and granule cell dematuration in the dentate gyrus. *Mol. Brain* 8, 29. <https://doi.org/10.1186/s13041-015-0120-3>.
- Janssen, P.A., Janssen, H., Cauwenbergh, G., De Doncker, P., De Beule, K., Lewi, P., Tytgat, H.F., Lapiere, C.M., 1989. Use of topical ketanserin in the treatment of skin ulcers: a double-blind study. *J. Am. Acad. Dermatol.* 21 (1), 85–90. [https://doi.org/10.1016/s0190-9622\(89\)70153-5](https://doi.org/10.1016/s0190-9622(89)70153-5).
- Jin, S.E., Seo, C.S., Jeon, W.Y., Oh, Y.J., Shin, H.K., Jeong, H.G., Ha, H., 2024. Evodiae Fructus extract suppresses inflammatory response in HaCaT cells and improves house dust mite-induced atopic dermatitis in NC/Nga mice. *Sci. Rep.* 14 (1), 472. <https://doi.org/10.1038/s41598-023-50257-3>.
- Kim, M.S., Pinto, S.M., Getnet, D., Nirujogi, R.S., Manda, S.S., Chaerkady, R., Madugundu, A.K., Kelkar, D.S., Isserlin, R., Jain, S., Thomas, J.K., Muthusamy, B., Leal-Rojas, P., Kumar, P., Sahasrabudhe, N.A., Balakrishnan, L., Advani, J., George, B., Renuse, S., Selvan, L.D., Patil, A.H., Nanjappa, V., Radhakrishnan, A., Prasad, S., Subbannayya, T., Raju, R., Kumar, M., Sreenivasamurthy, S.K., Marimuthu, A., Sathe, G.J., Chavan, S., Datta, K.K., Subbannayya, Y., Sahu, A., Yelamanchi, S.D., Jayaram, S., Rajagopalan, P., Sharma, J., Murthy, K.R., Syed, N., Goel, R., Khan, A.A., Ahmad, S., Dey, G., Mudgal, K., Chatterjee, A., Huang, T.C., Zhong, J., Wu, X., Shaw, P.G., Freed, D., Zahari, M.S., Mukherjee, K.K., Shankar, S., Mahadevan, A., Lam, H., Mitchell, C.J., Shankar, S.K., Satishchandra, P., Schroeder, J.T., Sirdeshmukh, R., Maitra, A., Leach, S.D., Drake, C.G., Halushka, M. K., Prasad, T.S., Hruban, R.H., Kerr, C.L., Bader, G.D., Iacobuzio-Donahue, C.A., Gowda, H., Pandey, A., 2014. A draft map of the human proteome. *Nature* 509 (7502), 575–581. <https://doi.org/10.1038/nature13302>.
- Kim, H.E., Cho, H., Ishihara, A., Kim, B., Kim, O., 2018. Cell proliferation and migration mechanism of caffeine/serotonin and serotonin via serotonin 2B receptor in human keratinocyte HaCaT cells. *BMB Rep* 51 (4), 188–193. <https://doi.org/10.5483/bmbrep.2018.51.4.209>.
- Kubera, M., Simbirsev, A., Mathison, R., Maes, M., 2000. Effects of repeated fluoxetine and citalopram administration on cytokine release in C57BL/6 mice. *Psychiatr. Res.* 96 (3), 255–266. [https://doi.org/10.1016/s0165-1781\(00\)00184-0](https://doi.org/10.1016/s0165-1781(00)00184-0).
- Laberge, S., Cruikshank, W.W., Beer, D.J., Center, D.M., 1996. Secretion of IL-16 (lymphocyte chemoattractant factor) from serotonin-stimulated CD8+ T cells in vitro. *J. Immunol.* 156 (1), 310–315. <https://www.ncbi.nlm.nih.gov/pubmed/8598478>.
- Lawrence, C.M., Matthews, J.N., Cox, N.H., 1995. The effect of ketanserin on healing of fresh surgical wounds. *Br. J. Dermatol.* 132 (4), 580–586. <https://doi.org/10.1111/j.1365-2133.1995.tb08714.x>.
- León-Ponte, M., Ahern, G.P., O'Connell, P.J., 2007. Serotonin provides an accessory signal to enhance T-cell activation by signaling through the 5-HT7 receptor. *Blood* 109 (8), 3139–3146. <https://doi.org/10.1182/blood-2006-10-052787>.
- Lyu, S., Chen, W., Qian, J., Wen, X., Xu, J., 2019. Prioritizing environmental risks of pharmaceuticals and personal care products in reclaimed water on urban green space in Beijing. *Sci. Total Environ.* 697, 133850. <https://doi.org/10.1016/j.scitotenv.2019.133850>.
- Macdonald, R.A., Robbins, S.L., Mallory, G.K., 1958. Dermal fibrosis following subcutaneous injections of serotonin creatinine sulphate. *Proc Soc Exp Biol Med* 97 (2), 334–337. <https://doi.org/10.3181/00379727-97-23734>.
- Marsden, A.J., Riley, D.R.J., Barry, A., Khalil, J.S., Guinn, B.A., Kemp, N.T., Rivero, F., Beltran-Alvarez, P., 2021a. Inhibition of arginine methylation impairs platelet function. *ACS Pharmacol. Transl. Sci.* 4 (5), 1567–1577. <https://doi.org/10.1021/acspctsci.1c00135>.
- Marsden, A.J., Riley, D.R.J., Birkett, S., Rodriguez-Barucg, Q., Guinn, B.A., Carroll, S., Ingle, L., Sathyapalan, T., Beltran-Alvarez, P., 2021b. Love is in the hair: arginine methylation of human hair proteins as novel cardiovascular biomarkers. *Amino Acids.* <https://doi.org/10.1007/s00726-021-03024-5>.
- Martin, J.M., Bertram, M.G., Saaristo, M., Ecker, T.E., Hannington, S.L., Tanner, J.L., Michelangeli, M., O'Bryan, M.K., Wong, B.B.M., 2019. Impact of the widespread pharmaceutical pollutant fluoxetine on behaviour and sperm traits in a freshwater fish. *Sci. Total Environ.* 650 (Pt 2), 1771–1778. <https://doi.org/10.1016/j.scitotenv.2018.09.294>.
- Martins, A.M., Ascenso, A., Ribeiro, H.M., Marto, J., 2020. The brain-skin connection and the pathogenesis of psoriasis: a review with a focus on the serotonergic system. *Cells* 9 (4). <https://doi.org/10.3390/cells9040796>.
- Michelangeli, M., Martin, J.M., Robson, S., Cerveny, D., Walsh, R., Richmond, E.K., Grace, M.R., Brand, J.A., Bertram, M.G., Ho, S.S.Y., Brodth, T., Wong, B.B.M., 2024. Pharmaceutical pollution alters the structure of freshwater communities and hinders their recovery from a fish predator. *Environ. Sci. Technol.* 58 (31), 13904–13917. <https://doi.org/10.1021/acs.est.4c02807>.

- Miranda, J.P.G.A., Isaac, A.B.J., Silva, R.B., Toledo, L.C.S., Barcellos, L.J.G., Delicio, H. C., Barreto, R.E., 2023. Acute effects of fluoxetine on stress responses and feeding motivation in Nile Tilapia. *Fishes* 8 (7). <https://doi.org/10.3390/fishes8070348>.
- Mokrzyński, K., Szewczyk, G., 2024. Photoreactivity of polycyclic aromatic hydrocarbons (PAHs) and their mechanisms of phototoxicity against human immortalized keratinocytes (HaCaT). *Sci. Total Environ.* 924, 171449 <https://doi.org/10.1016/j.scitotenv.2024.171449>.
- Mossner, R., Daniel, S., Schmitt, A., Albert, D., Lesch, K.P., 2001. Modulation of serotonin transporter function by interleukin-4. *Life Sci.* 68 (8), 873–880. [https://doi.org/10.1016/s0024-3205\(00\)00992-9](https://doi.org/10.1016/s0024-3205(00)00992-9).
- Nebigil, C.G., Etienne, N., Messaddeq, N., Maroteaux, L., 2003. Serotonin is a novel survival factor of cardiomyocytes: mitochondria as a target of 5-HT_{2B} receptor signaling. *FASEB J* 17 (10), 1373–1375. <https://doi.org/10.1096/fj.02-1122je>.
- Nguyen, C.M., Tartar, D.M., Bagood, M.D., So, M., Nguyen, A.V., Gallegos, A., Fregoso, D., Serrano, J., Nguyen, D., Degovics, D., Adams, A., Harouni, B., Fuentes, J. J., Gareau, M.G., Crawford, R.W., Soulika, A.M., Isseroff, R.R., 2019. Topical fluoxetine as a novel therapeutic that improves wound healing in diabetic mice. *Diabetes* 68 (7), 1499–1507. <https://doi.org/10.2337/db18-1146>.
- Nordlind, K., Azmitia, E.C., Slominski, A., 2008. The skin as a mirror of the soul: exploring the possible roles of serotonin. *Exp. Dermatol.* 17 (4), 301–311. <https://doi.org/10.1111/j.1600-0625.2007.00670.x>.
- Onwuli, D.O., Samuel, S.F., Sfyri, P., Welham, K., Goddard, M., Abu-Omar, Y., Loubani, M., Rivero, F., Matsakas, A., Benoit, D.M., Wade, M., Greenman, J., Beltran-Alvarez, P., 2019. The inhibitory subunit of cardiac troponin (cTnI) is modified by arginine methylation in the human heart. *Int. J. Cardiol.* 282, 76–80. <https://doi.org/10.1016/j.ijcard.2019.01.102>.
- Osaki, T., Shin, Y., Sivathanu, V., Campisi, M., Kamm, R.D., 2018. In vitro microfluidic models for neurodegenerative disorders. *Adv. Healthc. Mater.* 7 (2). <https://doi.org/10.1002/adhm.201700489>.
- Painter, M.M., Buerkley, M.A., Julius, M.L., Vajda, A.M., Norris, D.O., Barber, L.B., Furlong, E.T., Schultz, M.M., Schoenfeld, H.L., 2009. Antidepressants at environmentally relevant concentrations affect predator avoidance behavior of larval fathead minnows. *Environ. Toxicol. Chem.* 28 (12), 2677–2684. <https://doi.org/10.1897/08-556.1>.
- Pan, S.M., Zhou, Y.F., Zuo, N., Jiao, R.Q., Kong, L.D., Pan, Y., 2022. Fluoxetine increases astrocytic glucose uptake and glycolysis in corticosterone-induced depression through restricting GR-TXNIP-GLUT1 Pathway. *Front. Pharmacol.* 13, 872375 <https://doi.org/10.3389/fphar.2022.872375>.
- Payuhakrit, W., Panpinyaporn, P., Khumsri, W., Yusakul, G., Praphasawat, R., Nuengchamrong, N., Palipoch, S., 2024. Enhancing chronic wound healing with Thai indigenous rice variety, Kaab Dum: exploring ER stress and senescence inhibition in HaCaT keratinocyte cell line. *PLoS One* 19 (5), e0302662. <https://doi.org/10.1371/journal.pone.0302662>.
- Pinto, B., Correia, D., Conde, T., Faria, M., Oliveira, M., Domingues, M.D.R., Domingues, I., 2024. Impact of chronic fluoxetine exposure on zebrafish: from fatty acid profile to behavior. *Chemosphere* 357, 142026. <https://doi.org/10.1016/j.chemosphere.2024.142026>.
- Polter, A.M., Yang, S., Jope, R.S., Li, X., 2012. Functional significance of glycogen synthase kinase-3 regulation by serotonin. *Cell. Signal.* 24 (1), 265–271. <https://doi.org/10.1016/j.cellsig.2011.09.009>.
- Prasad, P., Ogawa, S., Parhar, I.S., 2015. Role of serotonin in fish reproduction. *Front. Neurosci.* 9, 195. <https://doi.org/10.3389/fnins.2015.00195>.
- Riley, A., Jones, H., England, J., Kuvshinov, D., Green, V., Greenman, J., 2021. Identification of soluble tissue-derived biomarkers from human thyroid tissue explants maintained on a microfluidic device. *Oncol. Lett.* 22 (5), 780. <https://doi.org/10.3892/ol.2021.13041>.
- Ritchie, M.E., Phipson, B., Wu, D., Hu, Y., Law, C.W., Shi, W., Smyth, G.K., 2015. Limma powers differential expression analyses for RNA-seq and microarray studies. *Nucleic Acids Res.* 43 (7), e47. <https://doi.org/10.1093/nar/gkv007>.
- Sadiq, A., Shah, A., Jeschke, M.G., Belo, C., Qasim Hayat, M., Murad, S., Amini-Nik, S., 2018. The role of serotonin during skin healing in post-thermal injury. *Int. J. Mol. Sci.* 19 (4) <https://doi.org/10.3390/ijms19041034>.
- Sahu, A., Gopalakrishnan, L., Gaur, N., Chatterjee, O., Mol, P., Modi, P.K., Dagamajalu, S., Advani, J., Jain, S., Keshava Prasad, T.S., 2018. The 5-Hydroxytryptamine signaling map: an overview of serotonin-serotonin receptor mediated signaling network. *J. Cell Commun. Signal* 12 (4), 731–735. <https://doi.org/10.1007/s12079-018-0482-2>.
- Salahinejad, A., Attaran, A., Meuthen, D., Chivers, D.P., Niyogi, S., 2022. Proximate causes and ultimate effects of common antidepressants, fluoxetine and venlafaxine, on fish behavior. *Sci. Total Environ.* 807 (Pt 2), 150846 <https://doi.org/10.1016/j.scitotenv.2021.150846>.
- Santos, L.H., Gros, M., Rodriguez-Mozaz, S., Delerue-Matos, C., Pena, A., Barcelo, D., Montenegro, M.C., 2013. Contribution of hospital effluents to the load of pharmaceuticals in urban wastewaters: identification of ecologically relevant pharmaceuticals. *Sci. Total Environ.* 461–462, 302–316. <https://doi.org/10.1016/j.scitotenv.2013.04.077>.
- Schlusener, M.P., Hardenbicker, P., Nilson, E., Schulz, M., Viergutz, C., Ternes, T.A., 2015. Occurrence of venlafaxine, other antidepressants and selected metabolites in the Rhine catchment in the face of climate change. *Environ. Pollut.* 196, 247–256. <https://doi.org/10.1016/j.envpol.2014.09.019>.
- Schneider, C.A., Rasband, W.S., Eliceiri, K.W., 2012. NIH Image to ImageJ: 25 years of image analysis. *Nat. Methods* 9 (7), 671–675. <https://doi.org/10.1038/nmeth.2089>.
- Seuwen, K., Magnaldo, I., Pouyssegur, J., 1988. Serotonin stimulates DNA synthesis in fibroblasts acting through 5-HT_{1B} receptors coupled to a Gi-protein. *Nature* 335 (6187), 254–256. <https://doi.org/10.1038/335254a0>.
- Silva, L.J., Lino, C.M., Meisel, L.M., Pena, A., 2012. Selective serotonin re-uptake inhibitors (SSRIs) in the aquatic environment: an ecopharmacovigilance approach. *Sci. Total Environ.* 437, 185–195. <https://doi.org/10.1016/j.scitotenv.2012.08.021>.
- Silva, L.J.G., Pereira, A., Meisel, L.M., Lino, C.M., Pena, A., 2015. Reviewing the serotonin reuptake inhibitors (SSRIs) footprint in the aquatic biota: uptake, bioaccumulation and ecotoxicology. *Environ. Pollut.* 197, 127–143. <https://doi.org/10.1016/j.envpol.2014.12.002>.
- Slominski, A., Pisarchik, A., Wortsman, J., 2004. Expression of genes coding melatonin and serotonin receptors in rodent skin. *Biochim. Biophys. Acta* 1680 (2), 67–70. <https://doi.org/10.1016/j.bbaexp.2004.09.002>.
- Sousa, M.A., Goncalves, C., Cunha, E., Hajslava, J., Alpendurada, M.F., 2011. Cleanup strategies and advantages in the determination of several therapeutic classes of pharmaceuticals in wastewater samples by SPE-LC-MS/MS. *Anal. Bioanal. Chem.* 399 (2), 807–822. <https://doi.org/10.1007/s00216-010-4297-0>.
- Sousa-Ferreira, L., Aveleira, C., Botelho, M., Alvaro, A.R., Pereira de Almeida, L., Cavadas, C., 2014. Fluoxetine induces proliferation and inhibits differentiation of hypothalamic neuroprogenitor cells in vitro. *PLoS One* 9 (3), e88917. <https://doi.org/10.1371/journal.pone.0088917>.
- Strimmer, K., 2008. fdrtool: a versatile R package for estimating local and tail area-based false discovery rates. *Bioinformatics* 24 (12), 1461–1462. <https://doi.org/10.1093/bioinformatics/btn209>.
- Szklarczyk, D., Kirsch, R., Koutrouli, M., Nastou, K., Mehryary, F., Hachilif, R., Gable, A. L., Fang, T., Doncheva, N.T., Pyysalo, S., Bork, P., Jensen, L.J., von Mering, C., 2023. The STRING database in 2023: protein-protein association networks and functional enrichment analyses for any sequenced genome of interest. *Nucleic Acids Res.* 51 (D1), D638–D646. <https://doi.org/10.1093/nar/gkac1000>.
- Tan, H., Polverino, G., Martin, J.M., Bertram, M.G., Wiles, S.C., Palacios, M.M., Bywater, C.L., White, C.R., Wong, B.B.M., 2020. Chronic exposure to a pervasive pharmaceutical pollutant erodes among-individual phenotypic variation in a fish. *Environ. Pollut.* 263 (Pt A), 114450 <https://doi.org/10.1016/j.envpol.2020.114450>.
- Tate, K., Kirk, B., Tseng, A., Ulfers, A., Litwa, K., 2021. Effects of the selective serotonin reuptake inhibitor fluoxetine on developing neural circuits in a model of the human fetal cortex. *Int. J. Mol. Sci.* 22 (19) <https://doi.org/10.3390/ijms221910457>.
- Vasskog, T., Berger, U., Samuelsen, P.J., Kallenborn, R., Jensen, E., 2006. Selective serotonin reuptake inhibitors in sewage influents and effluents from Tromsø, Norway. *J. Chromatogr. A* 1115 (1–2), 187–195. <https://doi.org/10.1016/j.chroma.2006.02.091>.
- Vaswani, M., Linda, F.K., Ramesh, S., 2003. Role of selective serotonin reuptake inhibitors in psychiatric disorders: a comprehensive review. *Prog. Neuro-Psychopharmacol. Biol. Psychiatry* 27 (1), 85–102. [https://doi.org/10.1016/s0278-5846\(02\)00338-x](https://doi.org/10.1016/s0278-5846(02)00338-x).
- Vindis, C., Cerretti, D.P., Daniel, T.O., Huynh-Do, U., 2003. EphB1 recruits c-Src and p25Shc to activate MAPK/ERK and promote chemotaxis. *J. Cell Biol.* 162 (4), 661–671. <https://doi.org/10.1083/jcb.200302073>.
- Wang, C.C., Man, G.C., Chu, C.Y., Borchert, A., Ugun-Klusek, A., Billett, E.E., Kuhn, H., Ufer, C., 2014. Serotonin receptor 6 mediates defective brain development in monoamine oxidase A-deficient mouse embryos. *J. Biol. Chem.* 289 (12), 8252–8263. <https://doi.org/10.1074/jbc.M113.522094>.
- Weinberger 2nd, J., Klaper, R., 2014. Environmental concentrations of the selective serotonin reuptake inhibitor fluoxetine impact specific behaviors involved in reproduction, feeding and predator avoidance in the fish *Pimephales promelas* (fathead minnow). *Aquat. Toxicol.* 151, 77–83. <https://doi.org/10.1016/j.aquatox.2013.10.012>.
- Welsh, D.J., Harnett, M., MacLean, M., Peacock, A.J., 2004. Proliferation and signaling in fibroblasts: role of 5-hydroxytryptamine_{2A} receptor and transporter. *Am. J. Respir. Crit. Care Med.* 170 (3), 252–259. <https://doi.org/10.1164/rccm.200302-2640C>.
- Wilkinson, H.N., Hardman, M.J., 2020. Senescence in wound repair: emerging strategies to target chronic healing wounds. *Front. Cell Dev. Biol.* 8, 773. <https://doi.org/10.3389/fcell.2020.00773>.
- Wilkinson, H.N., Longhorne, F.L., Roberts, E.R., Brownhill, V.R., Hardman, M.J., 2021. Cellular benefits of single-use negative pressure wound therapy demonstrated in a novel ex vivo human skin wound model. *Wound Repair Regen.* 29 (2), 298–305. <https://doi.org/10.1111/wrr.12888>.
- Woodman, S.G., Steinkey, D., Dew, W.A., Burket, S.R., Brooks, B.W., Pyle, G.G., 2016. Effects of sertraline on behavioral indices of crayfish. *Ecotoxicol. Environ. Saf.* 134, 31–37. <https://doi.org/10.1016/j.ecoenv.2016.08.011>.
- Yoon, D.J., Nguyen, C., Bagood, M.D., Fregoso, D.R., Yang, H.Y., Medina Lopez, A.I., Crawford, R.W., Tran, J., Isseroff, R.R., 2021. Topical fluoxetine as a potential nonantibiotic adjunctive therapy for infected wounds. *J. Invest. Dermatol.* 141 (6), 1608. <https://doi.org/10.1016/j.jid.2020.11.016>, 1612 e1603.
- Yuksel, E.P., Ilkaya, F., Yildiz, L., Aydin, F., Senturk, N., Denizli, H., Canturk, T., Turanlı, A.Y., 2014. Effects of paroxetine on cutaneous wound healing in healthy and diabetic rats. *Adv. Skin Wound Care* 27 (5), 216–221. <https://doi.org/10.1097/01.ASW.0000445920.14039.64>.
- Zamani, A., Qu, Z., 2012. Serotonin activates angiogenic phosphorylation signaling in human endothelial cells. *FEBS Lett.* 586 (16), 2360–2365. <https://doi.org/10.1016/j.febslet.2012.05.047>.
- Zavaritskaya, O., Lubomirov, L.T., Altay, S., Schubert, R., 2017. Src tyrosine kinases contribute to serotonin-mediated contraction by regulating calcium-dependent

- pathways in rat skeletal muscle arteries. *Pflugers Arch* 469 (5–6), 767–777. <https://doi.org/10.1007/s00424-017-1949-3>.
- Zhang, Y.Q., Gao, X., Ji, G.C., Huang, Y.L., Wu, G.C., 2001. Expression of 5-HT_{2A} receptor mRNA in rat nucleus raphe magnus neurons after peripheral inflammation. *Acta Pharmacol. Sin.* 22 (10), 923–928. <https://www.ncbi.nlm.nih.gov/pubmed/11749776>.
- Zheng, Y., Zhang, W., Pendleton, E., Leng, S., Wu, J., Chen, R., Sun, X.J., 2009. Improved insulin sensitivity by calorie restriction is associated with reduction of ERK and p70S6K activities in the liver of obese Zucker rats. *J. Endocrinol.* 203 (3), 337–347. <https://doi.org/10.1677/JOE-09-0181>.